Received: 24 November 2021 | Revised: 2 June 2022 | Accepted: 3 June 2022

DOI: 10.1002/esp.5430

RESEARCH ARTICLE

ESPL WILEY

Subglacial evolution from distributed to channelized drainage: Evidence from the Lake Murtoo area in SW Finland

Antti E. K. Ojala[1] | Joni Mäkinen[1] | Kari Kajuutti[1] | Elina Ahokangas[1] | Jukka-Pekka Palmu[2]

[1]Department of Geography and Geology, University of Turku, Turku, Finland

[2]Geological Survey of Finland, Espoo, Finland

Correspondence
Antti Ojala, Department of Geography and Geology, University of Turku, Turku FI-20014, Finland.
Email: aneoja@utu.fi

Funding information
Academy of Finland, Grant/Award Numbers: 322243, 322252

Abstract

During the last millennia of the Weichselian glaciation (c. 11 700–14 000 cal BP) and the first millennium of the Holocene interglacial (c. 10 500–11 700 cal BP), melting of the ice sheet and subsequent subglacial drainage resulted in the formation of murtoos and murtoo-related landforms in the Fennoscandian Ice Sheet area in Finland and Sweden. Murtoos are composed of clay-poor diamictons produced by sediment-concentrated creep and material sorting in a subglacial environment under effective pressure close to zero, and potentially represent a transition form from non-channelized to channelized subglacial drainage networks. Here, we explore the geomorphology and substratum characteristics of the Lake Murtoo area, one of the locations where murtoos were initially found and described in SW Finland. Our interpretation suggests an interconnected development from inefficient distributed or semi-distributed cavities (murtoos) to efficient channelized drainage (esker) via erosional escarpments, all displayed in the same region. In addition, our excavation into a murtoo-related erosional escarpment (MRE) revealed subglacial erosional channels alongside MREs that were filled with fine-grained finely laminated sediments. We suggest that these channel fill sediments were deposited subglacially, because they are covered by flow till and show spatial and lithological characteristics that deviate significantly from the proglacial basin fill clay (varve) sediments in the area. The appearance of rhythmically laminated silt and clay sediments indicates sedimentation in a suspension-load-dominated environment in shallow subglacial channels with relatively low (but repetitiously changing) water flow velocities, possibly reflecting disconnected spill-over routes of subglacial drainage in small tributaries that were only periodically used due to water pressure changes in the up-ice direction.

KEYWORDS
Fennoscandian Ice Sheet, Finland, glacial sediment, laminated sediment, murtoo, subglacial drainage

1 | INTRODUCTION

Glacial landscapes offer insights into subglacial processes that erode, transport, and deposit sediments during glacial cycles (Hall et al., 2020; Menzies et al., 2018; Möller & Dowling, 2018). The formation and morphological characteristics of subglacial landforms vary in space and time, depending on the ice sheet–sediment association (rigid or deforming bed), bed topography, ice sheet velocity, basal shear stress, and subglacial hydrology, including effective pressure (e.g. Boulton et al., 2001; Hart, 1995). Subglacial hydrological networks in both distributed (inefficient) and channelized (efficient) environments contribute to subglacial drainage and sediment distribution underneath active ice lobes (e.g. Bowling et al., 2019; Davison et al., 2019; Lewington et al., 2020; Ojala et al., 2019, 2021). Moreover, the variety and

complexity of subglacial processes, as well as the production, storage, and pressure of subglacial meltwater, can lead to oscillations and spatiotemporal behaviour of glaciers (Bartholomaus et al., 2008; Clarke, 2005; Fricker et al., 2007; Mejia et al., 2021). Studies that demonstrate spatial and temporal relationships between subglacial drainage and deposition of sediments are important for reconstructing the growth and decay of paleo-ice sheets and the genesis of glacial landforms (e.g. Boulton et al., 2001; Clark et al., 2012), as well as for understanding the mechanisms by which modern glaciers will behave in the current warming climate (Cuffey & Paterson, 2010; Mejia et al., 2021).

Recent findings have suggested that landforms called murtoos were formed subglacially in the transition zone between distributed (sheets and films, cavities) and channelized drainage, and in places where the bed of the Fennoscandian Ice Sheet (FIS) received repeated influxes of meltwater during deglaciation (Mäkinen et al., 2019; Ojala et al., 2019, 2021; Peterson Becher & Johnson, 2021). In a nationwide mapping programme in Finland, Ahokangas et al. (2021) demonstrated that the formation of murtoos along subglacial meltwater corridors was dictated by the marked concentration and routing of subglacial meltwater in association with subglacial tunnel flow and zones of channelized drainage (eskers). Moreover, interbedded characteristics of murtoo sediments indicate that they were formed in a dynamic environment where glacially driven deformation and the input of large but brief pulses of meltwater to the ice sheet bed periodically fluctuated (Peterson Becher & Johnson, 2021). Such an environment and processes are similar to present-day Greenland and Antarctica, where global warming is causing changes in glacial hydrology and dynamics (e.g. Davison et al., 2019; Doyle et al., 2021; Fricker et al., 2007).

Based on their morphometric characteristics, Ojala et al. (2021) classified murtoos into common and widespread types in the Finnish area of the FIS. They demonstrated that in addition to triangle-type (TTM), chevron-type (CTM) and lobate-type murtoos (LTM), murtoo fields often contain murtoo-related ridges and escarpments (MRE). The shape and size of the escarpments are often similar to the shape of the murtoo edges. At places, MREs exhibit diagonal or curvilinear characteristics and form hundreds of metres long channel-like passages with erosional characteristics. Ojala et al. (2021) proposed that extensive MREs could actually represent pathways that guided hydrological routing along which subglacial meltwater was evacuated towards the R-channels (Boulton & Hindmarsh, 1987; Röthlisberger, 1972), whereas TTMs, CTMs, and LTMs represent more advanced forms of subglacial sediment saturation, progressive creep, and deposition.

In this paper, we describe field sections of the trench excavations of an MRE in the vicinity of Murtoo village, in SW Finland. The Lake Murtoo area is particularly interesting, because it is characterized by a geomorphological transition from TTMs to the onset of the Rämsöö–Hämeenlinna esker via MREs. Our focus is on the description of MRE lithofacies in order to understand the processes responsible for the formation of these landforms. By combining MRE lithofacies (sediment textural and structural characteristics) with regional LiDAR-based geomorphology and drilling, we then consider how a subglacial meltwater route evolves from TTMs (semi-distributed) to an esker (channelized) via MREs.

2 | GEOLOGICAL SETTING

The study area was subjected to multiple glaciations during the Pleistocene epoch. The extent and dynamics of the FIS for the most recent glacial stage (the Weichselian glaciation) are well constrained by geomorphological evidence and the compilation of radiocarbon, luminescence, and cosmogenic isotope ages (e.g. Batchelor et al., 2019; Boulton et al., 2001; Hughes et al., 2016; Rainio et al., 1995; Rinterknecht et al., 2018; Stroeven et al., 2016; Svendsen et al., 2004). During the Late Weichselian glacial maximum (23–19 cal ka BP), the FIS covered all of Fennoscandia and extended to northern Germany and NW Russia. By the end of the Weichselian, the retreating FIS was divided into several active ice lobes in Finland that operated time-transgressively in response to the Late Weichselian and Early Holocene climate fluctuations (Boulton et al., 2001; Kleman et al., 1997; Punkari, 1980) (Figure 1). Still-stands and re-advances of the ice lobes formed large ice-marginal formations throughout Finland and NW Russia, including the Salpausselkä complexes (Ss I, Ss II, Ss III) in southern Finland (Lunkka et al., 2021; Rainio et al., 1995).

The present study area lies within the area covered by the Baltic Sea Ice Lobe up-ice from Ss III and was deglaciated at around 11 cal ka BP during the Yoldia Sea phase in the Baltic Sea basin (BSB) history (Björck, 1995; Palmu et al., 2021; Stroeven et al., 2016). The northeastern sector of the Baltic Sea Ice Lobe disintegrated from the main lobe during the rapid melting of the ice sheet after formation of the Ss III complex, forming the Loimaa sublobe (Mäkinen, 2003). The Säkylä–Virttaankangas esker complex and the Tampere–Kangasala–Pälkäne esker indicate the largest subglacial meltwater routes in the area (Figure 1). These two eskers were formed at the interlobate margins of the Loimaa sublobe and the lobes to the NE and SW. The Kokemäenjoki River Valley, including largely the Kulovesi and Rautavesi lakes, is roughly transverse to the ice-flow direction and nowadays draining towards the west. The river valley was probably a large subglacial lake during deglaciation, which provided meltwater for a central subglacial drainage system of the Loimaa sublobe and divided it into southeastern and northwestern areas that are geomorphologically different (Ahokangas et al., 2021) (Figure 1).

The study area contains numerous murtoo, ribbed, and hummocky moraine fields and most of them are associated with eskers and other subglacial meltwater routes (Ahokangas et al., 2021) (Figure 1). In the Baltic Sea Ice Lobe area, murtoos only occur along the northeastern margin (i.e. in the Loimaa sublobe area) (Ojala et al., 2019). Murtoo fields are composed of TTMs, CTMs, and MREs (Ojala et al., 2021). Glacial lineations appear in swarms and are composed of flutings, drumlins, and drumlinoids, and reflect active ice-flow areas during the Late Weichselian. The absence of murtoo fields in areas of glacial lineations is clear. Glacial lineations and striations indicate two main ice-flow directions, 275–290° towards the Ss III phase and 315–320°, which are older and point towards the Last Glacial Maximum.

Exposed and in places steep bedrock outcrops are numerous in the study area (Figure 2). The bedrock belongs to Paleoproterozoic supracrustal and plutonic rocks of Svecofennia, formed 1.78–1.93 Ga ago (Lahtinen, 1996) and consisting of biotite paragneiss and granodiorite of the Pirkanmaa migmatite suite, which extends 320 km in an E–W direction across the region. Bedrock and glacial landforms in the Lake Murtoo vicinity are partially overlain by clayey sediments of the BSB and scattered peat deposits, which are seen as flat areas at a lower elevation (<100 m a.s.l.) (Figure 2). The highest shoreline in the study area lies at 155 m a.s.l. (Ojala et al., 2013).

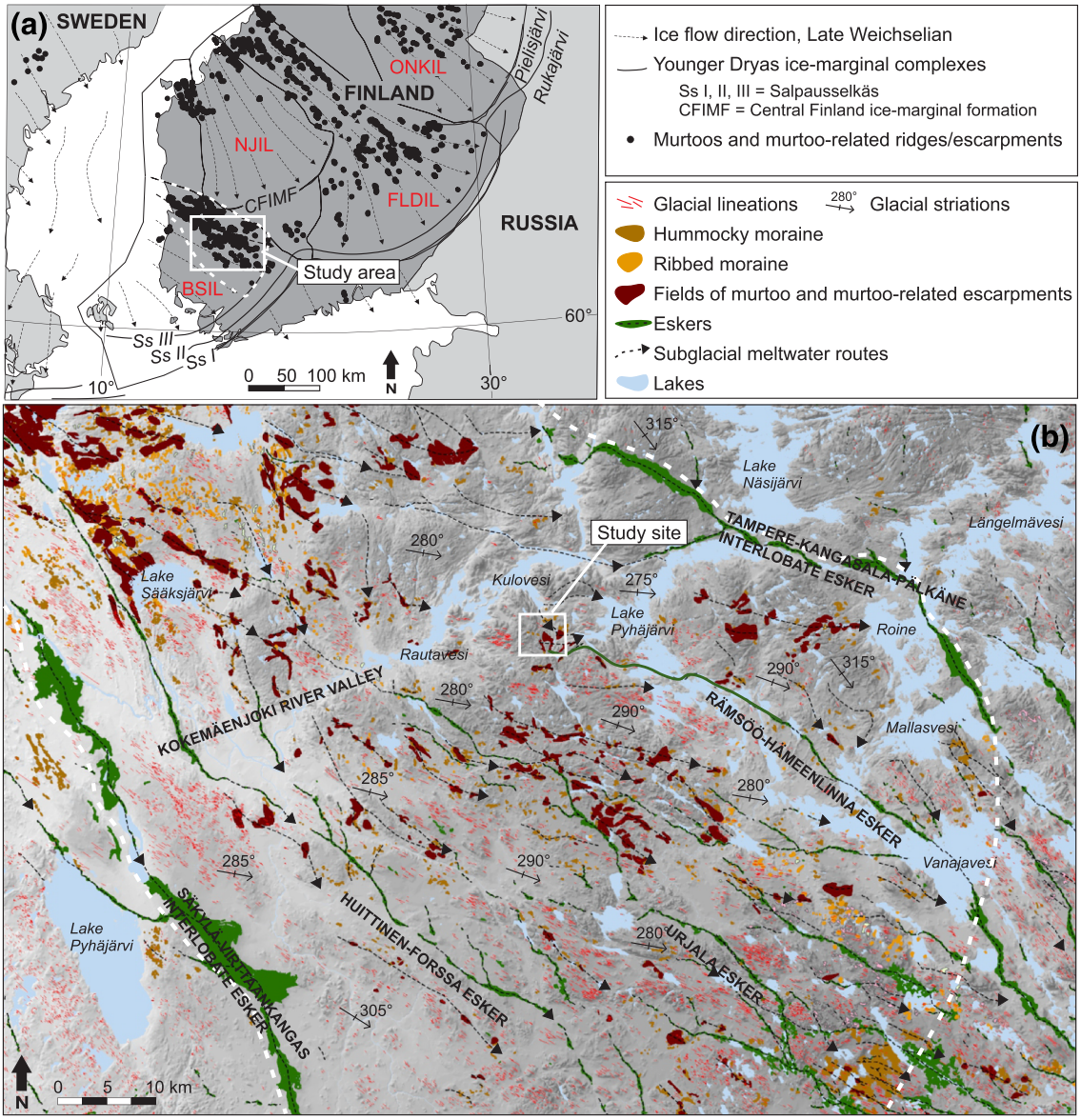

FIGURE 1 (a) Location of the study area in the Baltic Sea ice lobe with the spatial distribution of murtoos and murtoo-related landforms in NE Sweden and Finland (Ojala et al., 2019, 2021). Solid black lines indicate younger Dryas ice-marginal complexes, the Salpausselkäs (Ss I, Ss II, Ss III), and the Central Finland ice-marginal formation (CFIMF) (Hughes et al., 2016; Rainio et al., 1995). Dashed lines with arrows are the main flow lines of ice streams during the Weichselian deglaciation (Boulton et al., 2001; Kleman et al., 1997; Palmu et al., 2021; Rainio et al., 1995), with red letters indicating glacial dynamic provinces: BSIL = Baltic Sea ice lobe, FLDIL = Finnish Lake District ice lobe, NJIL = Näsijärvi–Jyväskylä ice lobe, ONKIL = Oulu–North-Karelia ice lobe. (b) Hillshaded DEM of the study area with selected Late Pleistocene glacial characteristics and meltwater routes, eskers, and modern lake basins. Dashed white line indicate the boundaries of the Loimaa sublobe in the BSIL area.

3 | MATERIALS AND METHODS

Glacial sequences and landforms in the Lake Murtoo area were surveyed by mapping from LiDAR digital elevation models (DEMs), trenching field sections, and drilling through Quaternary sediments (Figure 2). The main trench section (TE1), which was 50 m long, 3–4 m wide, and up to 4 m deep, was excavated perpendicular to an extensive escarpment (MRE) to reveal the sediment structures and material characteristics (Figure 2). The thickness and geometry of lithofacies were also revealed from a shorter and parallel excavation, TE2 (7.5 m long), located downslope of the escarpment. Remote sensing data were supplemented with a field mapping of superficial deposits using hand-driven probing.

The vertical field sections of the excavations were photographed and logged for detailed lithology and sedimentary structures, including grain-size analysis (Udden-Wentworth scale), clast roundness (Powers, 1953), and stone percentage counts. The logging also included measurements of tilting and direction of laminae sets and measurements of the diamicton macrofabrics (50 clasts, azimuth and dip) (Evans & Benn, 2004). The grain-size distribution of lithofacies units was based on 22 samples (TE1/1–21, TE2/22) that were dry sieved in the laboratory and measured for the fine-grained fraction (<0.063 mm) using a Micromeritics SediGraph III Plus with MasterTech 52 autosampler.

In order to compare the sediment characteristics of clay and silt-filled channels (Log2) found in the trenched section TE1 with fine-grained deposits of the BSB on the Lanajoki River Valley floor, we

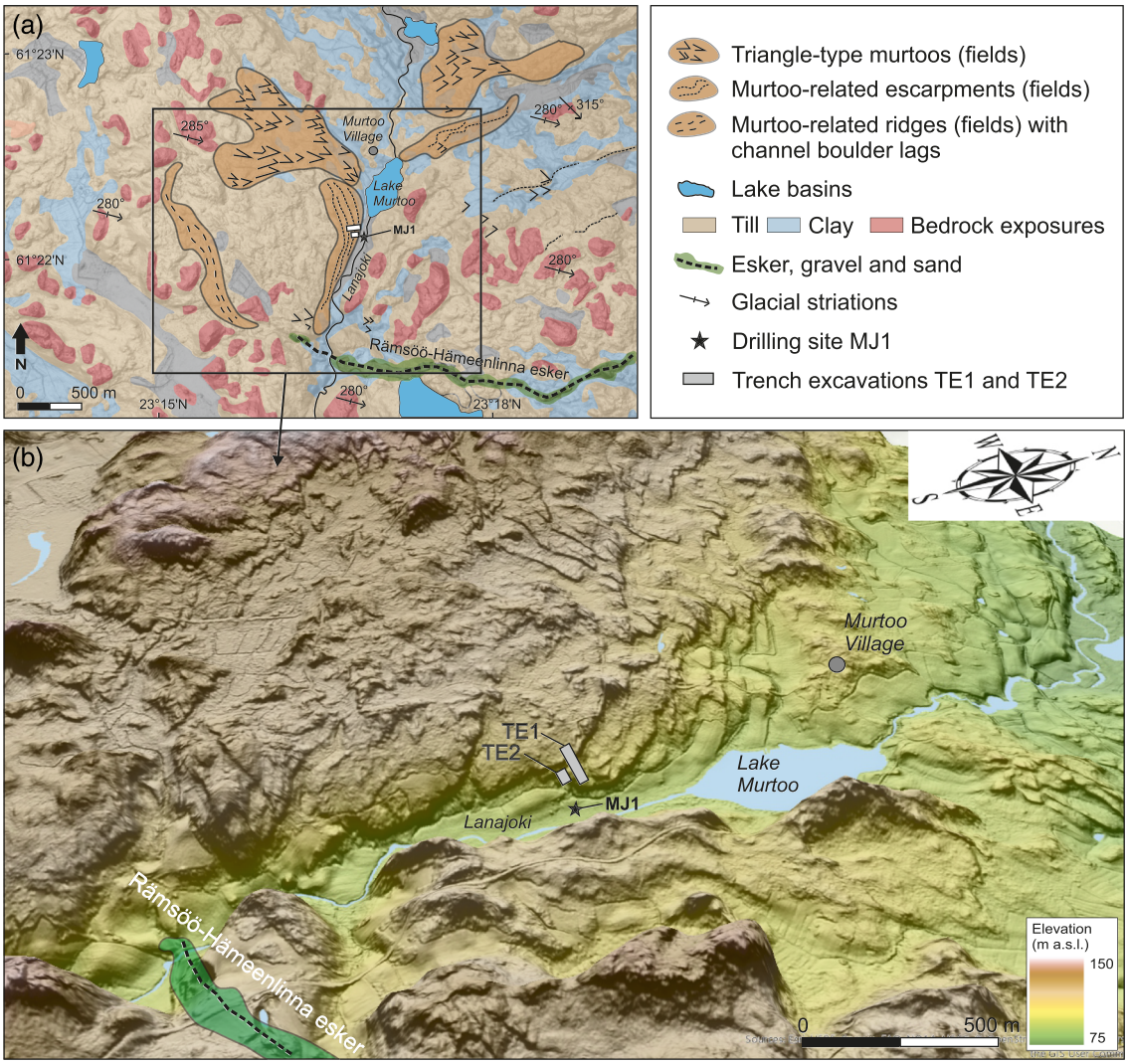

FIGURE 2 (a) The Lake Murtoo study site on a map of quaternary deposits. The terrain is composed of till and bedrock outcrops, and the lowest-lying areas (<100 m a.s.l.) are clay-covered. A field of TTMs leads to the onset of the Rämsöö–Hämeenlinna esker via erosional MREs located on the western side of the Lanajoki River valley. (b) Three-dimensional LiDAR-based DEM of the study site with the locations of trench excavations TE1 and TE2 and coring site MJ1 on the valley floor.

drilled a borehole (MJ1) in the bottom of the valley (95.0 m a.s.l.) about 200 m S–SW of Lake Murtoo (Figure 2). A comparison of fine-grained facies in channels alongside MREs (Log2) and in the bottom of the valley (MJ1) is an essential part of the study, in order to discriminate their sedimentation environment. Sediment units recognized in the Log2 and MJ1 sections were identified and described in detail for sediment structures and lithological components according to the classification of Troels-Smith (1955). Both sections were then analysed for loss on ignition (LOI) and magnetic susceptibility. LOI measurements were performed according to Håkanson and Jansson (1983) and we used a Bartington MS2E1 surface scanning sensor to record magnetic susceptibility at 2–3 cm resolution.

4 | RESULTS AND INTERPRETATION

4.1 | Regional geomorphology

Based on LiDAR DEMs, the Lake Murtoo study area consists of several locations where scattered murtoos or fields of murtoos appear and are spatially associated with subglacial meltwater systems and MREs (Figure 2a). The murtoo fields and meltwater routes in the Lake Murtoo area occur distal to the Kokemäenjoki River Valley, which was probably occupied by large subglacial lakes during deglaciation (Figure 1b). The topographic connection to Kulovesi lies directly north of the present study site. There are no eskers or subglacial meltwater routes up-ice from the Lake Murtoo area (i.e. between the Kokemäenjoki River Valley and the present study site; Figure 1b). Instead, in the down-ice direction (southeast) is the Rämsöö–Hämeenlinna esker that extends through Lake Pyhäjärvi and towards the Vanajavesi basin. The area between the Rämsöö–Hämeenlinna esker and the Tampere–Kangasala–Pälkäne interlobate esker forms the northern edge of the Vanajavesi ice-flow system, which is associated with lineation fields indicating ice-flow direction until Ss I.

The spatial distribution of murtoo fields and subglacial meltwater routes in the Lake Murtoo vicinity indicate manifold and probably time-transgressive shifting of subglacial drainage during deglaciation (Ahokangas et al., 2021). One route of subglacial drainage is from the Kulovesi basin towards the Lake Pyhäjärvi basin (Figure 1b). Another subglacial meltwater route from the Kulovesi basin is towards the

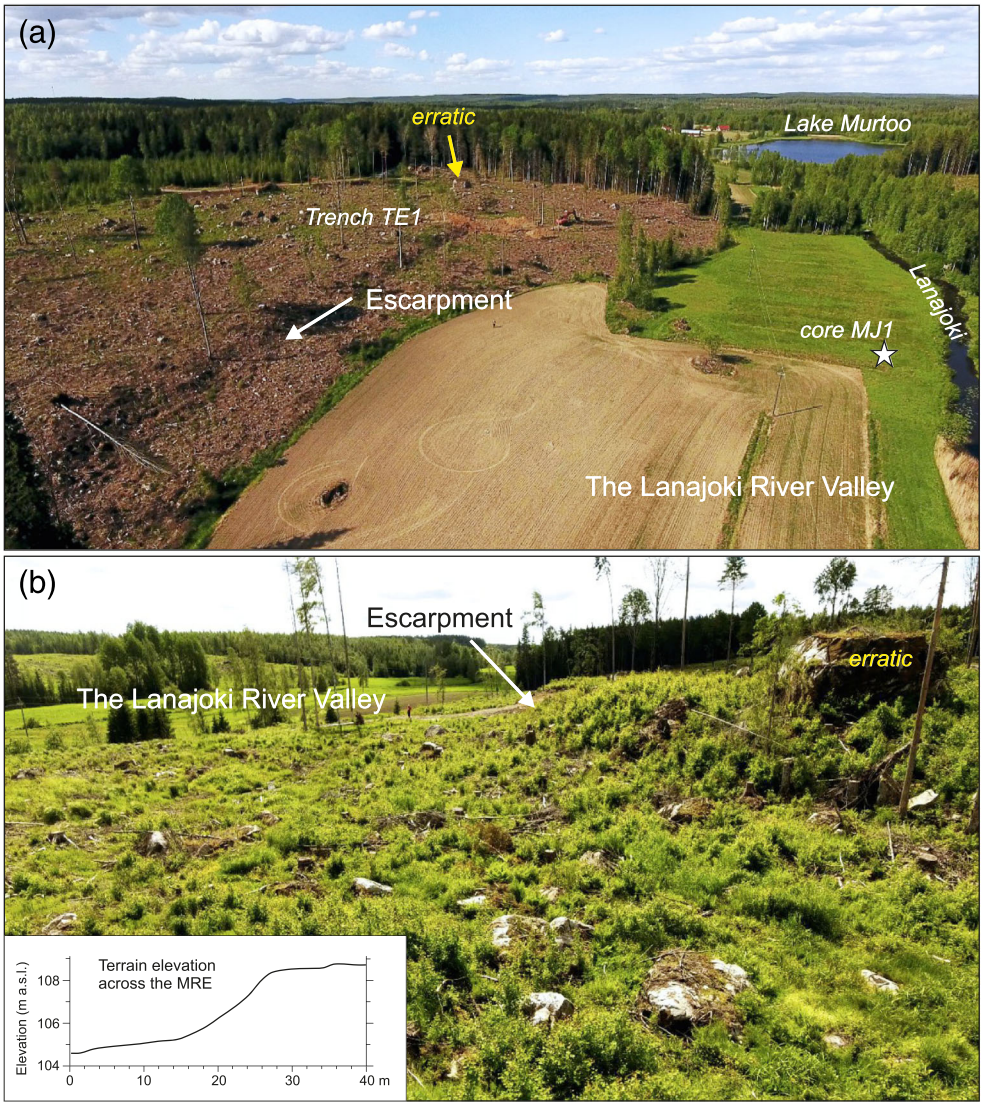

FIGURE 3 Photographs (taken with a drone) of the MRE south of Lake Murtoo. The escarpment, which is hundreds of metres long and several metres high, is clearly visible alongside the Lanajoki River valley because of recent forest clear-cutting. Note the frequency of surface boulders in the study area with the same 3 m-high glacial erratic marked in both photographs (a, b). Trench TE1 was excavated to cross-cut the MRE perpendicularly; observe the 40 ton excavator in the lower part of the trench for scale. The coring site MJ1 on the valley floor is marked on A and the terrain elevation profile perpendicularly across the MRE is from the location indicated by a white arrow in B. (Photographs are looking towards the north for A and towards the south for B.)

south and the onset of the Rämsöö–Hämeenlinna esker via the Lanajoki River Valley. When deglaciation proceeded, meltwaters also flowed out from the Rautavesi basin towards the south and southeast (i.e. towards the Urjala esker; Figure 1b).

Of particular interest in the Lake Murtoo study area is a geomorphological transition from TTMs to the onset of the Rämsöö–Hämeenlinna esker via MREs (Figure 2a). This continuum begins from an extensive field of murtoos that appears west of Lake Murtoo, with murtoo tip angles pointing in the latest ice-flow direction. The murtoo field contains ~35 forms and partially overlapping TTMs (Ojala et al., 2021). The murtoo field terminates at Lake Murtoo in the east and connects to escarpments (MREs) that turn southwards alongside the Lanajoki River Valley. There are six parallel to subparallel and subequally spaced escarpments that are several hundred metres long, which can be traced alongside the bedrock fracture valley. MREs exhibit curvilinear and erosional characteristics. MREs are related to murtoos because they occur near them and murtoo edges have similar morphologies to the escarpments. Escarpments are up to 5 m high, exhibit terrace-like morphologies, and are covered by large boulders and glacial erratics (Figure 3). In the lower-lying areas, parts of these MREs are covered by postglacial clay and peat, especially in the Lanajoki River Valley. Escarpments terminate at the onset of the Rämsöö–Hämeenlinna esker in the southern part of the valley.

4.2 | Lithofacies of the MRE

Sediment excavated across the MRE was divided into four depositional units (Units 1–4) defined by their boundaries and the sedimentary architecture (Figure 4).

The bottom-most Unit 1 is composed of poorly sorted, sandy, massive, and matrix-supported to crudely stratified gravel [G(s)mm/cs, G(s)cs] (Figures 5e and 6, Table 1). Stratification includes crude troughs about 0.5–1.5 m wide and 0.2–0.5 m high, indicating ice flow towards the SSE. The gravel is highly mixed and resembles sandy and crudely stratified diamicton with a very low clay content and occasional small boulders (see Supplementary Data S1–S4). The gravel is also interbedded with partly preserved sand beds and lenses that contain contorted laminations (S[g]l). A general dip direction of the uppermost sand bed is towards the SSE (160–165°), with dips of 11–12°. The percentage of cobbles and boulders is low and ranges between 5 and 10%. Clasts are dominantly subangular to subrounded. The gravel facies becomes more deformed [G(s)mm/d] towards the steeper slope of the escarpment, where it is also partly mixed with and deformed by the overlying diamicton of Unit 2 (Log3, Figures 4a and 6). In the lower part of the escarpment (closer to the valley) there are channels cut into Unit 1 that are filled with sediment of Unit 3. Gravelly Unit 1 is generally 2–4 m thick and in contact with the

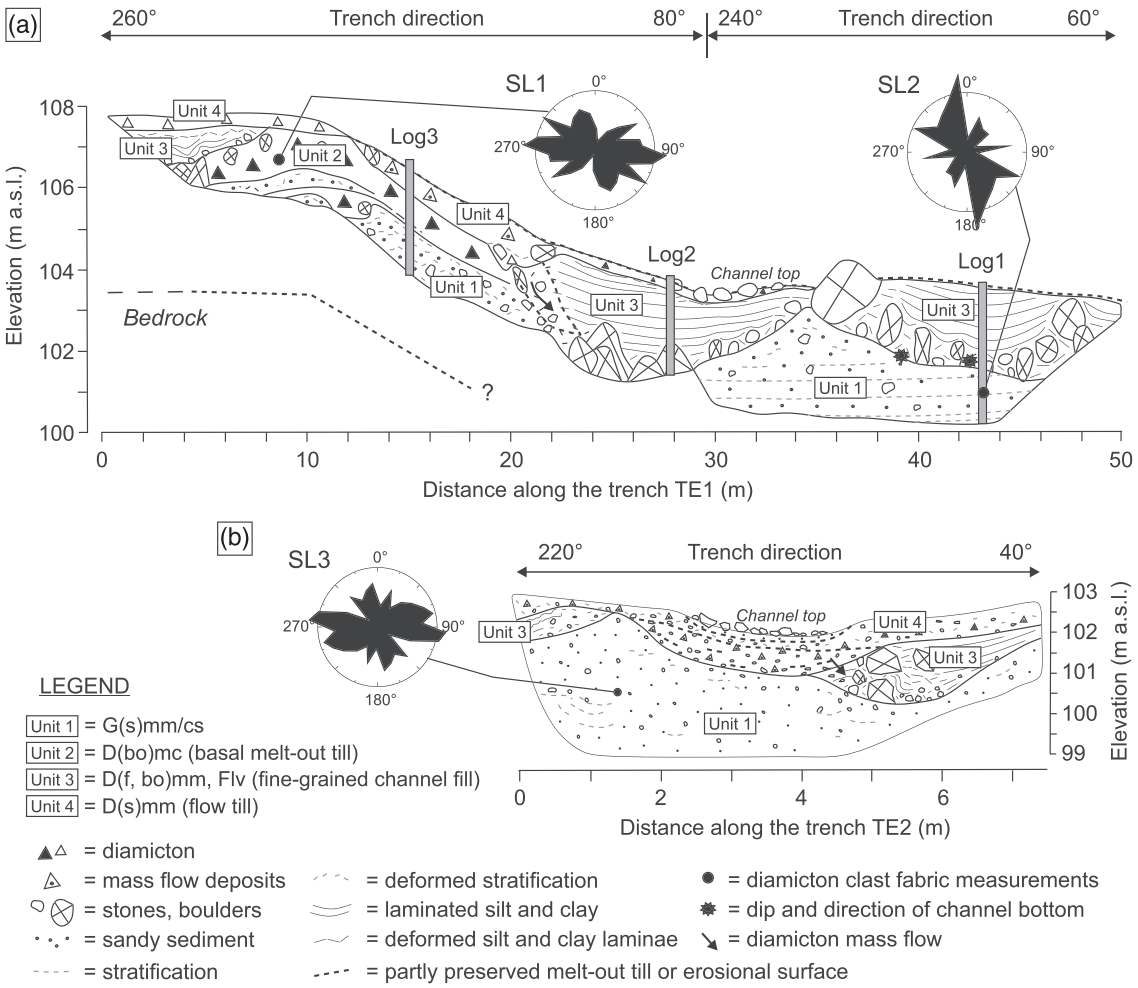

FIGURE 4 Profiles of the trench excavations TE1 (a) and TE2 (b) showing the subsurface geometry of lithofacies Units 1–4, macro-fabric directions, and the locations of sections Log1, Log2, and Log3 across an MRE at the Lake Murtoo study site (see Figure 2 for the locations of excavations).

bedrock probably at a level of 100–105 m a.s.l. in the upper section of the escarpment, based on the appearance of bedrock outcrops in the Lanajoki River Valley (Figures 2a, 4, and 6).

Unit 1 is interpreted to represent deposition of sediments in actively evolving subglacial conduits and cavities. This environment displays basal sediment erosion and mass-flow-type sediment accommodation of high-sediment-concentration flows through the subglacial hydrological system. The flow was directed along the Lanajoki River Valley, as indicated by clast macro-fabrics (SL2 in Figure 4a). Sand beds and lenses within massive gravel-dominated diamicton represent tranquil subglacial water flows, which became mixed by repeated pulses of sediment-concentrated flows. The sediment composition and interbedded characteristics resemble sediments in the lower part ('body') of murtoos and MREs, as described by Mäkinen et al. (2017, 2019), Ojala et al. (2021), and Peterson Becher and Johnson (2021). Unit 1 was deposited in an enlarged subglacial cavity and in association with glacially driven deformation and water flowing in cavities between the ice and the underlying bed.

Unit 2 is composed of bouldery, massive, and matrix- to clast-supported diamicton [D(bo)mc, D(f,bo)mm] with a clast content of about 20–35% (Figures 5f and 6, Table 2). The diamicton is 1–2 m thick and slightly compact without significant deformation. It contains poorly preserved sand patches and gravel interbeds, similar to Unit 1. The clasts are dominantly angular to subangular. The largest boulders are ~1 m in diameter and are located in the upper part of the exposure (Figure 6). Unit 2 is missing from the lower part of the escarpment but forms the deformed western margin of the channel (Unit 3) at the steepest slope.

Unit 2 is interpreted as basal melt-out till, indicating ice flow from the west and over the escarpment (S1 in Figure 4a). This direction corresponds to the latest local ice-flow direction indicated by bedrock striations (275–280°) and glacial lineations (Figure 1). A melt-out origin is supported by the stratified appearance of discontinuous and contorted inter-till layers and lenses of sand and gravel, which have indistinct contacts and internal flow structures (Evans et al., 2006; Shaw, 1982). Thickening and draping characteristics of sorted sediments over larger clasts are typical for Unit 2, which is a diagnostic feature for melt-out processes due to differential vertical settling of sediment (Evans et al., 2006). Low compaction and low deformation indicate that sediment is released by the melting of slowly moving (or stagnant) debris-rich glacier.

Unit 3 includes sediments in channels carved into lower-lying units (Figures 4 and 5a–c). Three of the channels were exposed in trench excavations TE1 and TE2. In general, the channels are about 2–3 m deep and 10–15 m wide, and their base is composed of sand and gravel with outsized clasts and large boulders [D(f,bo)mm]

FIGURE 5 Selected photographs of surface geomorphology and subsurface characteristics of the MRE in excavation TE1 at the Lake Murtoo study site (see Figure 2 for the location of TE1). (a) Channels filled with fine-grained sediments (Unit 3) run parallel to the Lanajoki River valley and at the toe of an escarpment (photo looking towards the south). (b) The base of Unit 3 is composed of sandy sediments with clasts and large boulders (Sub-unit 3a) and filled with laminated clay and silt (Sub-units 3b–3f). (c) Contact between Sub-units 3a and 3b has an undulating character. (d) Channel-fill sediments (Unit 3) clearly indicate rhythmic sedimentation patterns, with a number of silty laminae within each set of Sub-unit 3c. (e) Typical crudely stratified gravel with sand of Unit 1. Note the lack of larger clasts in this unit. (f) Clast-rich facies of Unit 2 interlayered by more sandy facies in the upper part of the trench TE1.

(Unit 3a) (Figure 6, Table 1). Large boulders up to 2 m in diameter lie in the middle of the channel bottom at the toe of the slope (Figure 5b). The entire trough-shaped channel bottoms are covered by a crude lag of clasts, typically 1–3 clasts thick (Figure 4). These clasts are subangular to subrounded. The channels are filled with rhythmically laminated to bedded clay and silt with occasional small pebbles (Units 3b–f). Laminations are conformable over large boulders at the bottom. All the channels show similar fills, with the thickest sediment fill in the middle of the channel and with draped characteristics. The detailed characteristics and sediment structures of this unit are described in the following section (Log2 in Figure 4a). It is noteworthy that the uppermost channel in the TE1 excavation shows signs of plastic deformation of contorted fine-grained beds throughout the unit, whereas in the lower-lying locations only the uppermost ~50 cm has been plastically deformed by the overlying Unit 4.

Unit 3 is interpreted to represent an interrelated sequence of erosion and deposition in subglacial channels alongside the MRE. The base of Unit 3 is an erosional surface carved into Unit 1 during widening and channelization of the subglacial meltwater flow, which would have occurred closer to the ice margin compared with the formation of Unit 1 and murtoos up-ice. Large boulders at the bottom of channels indicate rapid expansion of conduit roofs and mixing of boulders with channel bottom fines and sands in a high-flow meltwater environment. The initiation of the channels was rapidly followed by diminishing water flows along all the channels and deposition of rhythmically laminated channel fills denoting low-energy water-lain deposition (Figure 5d). Occasional pebbles

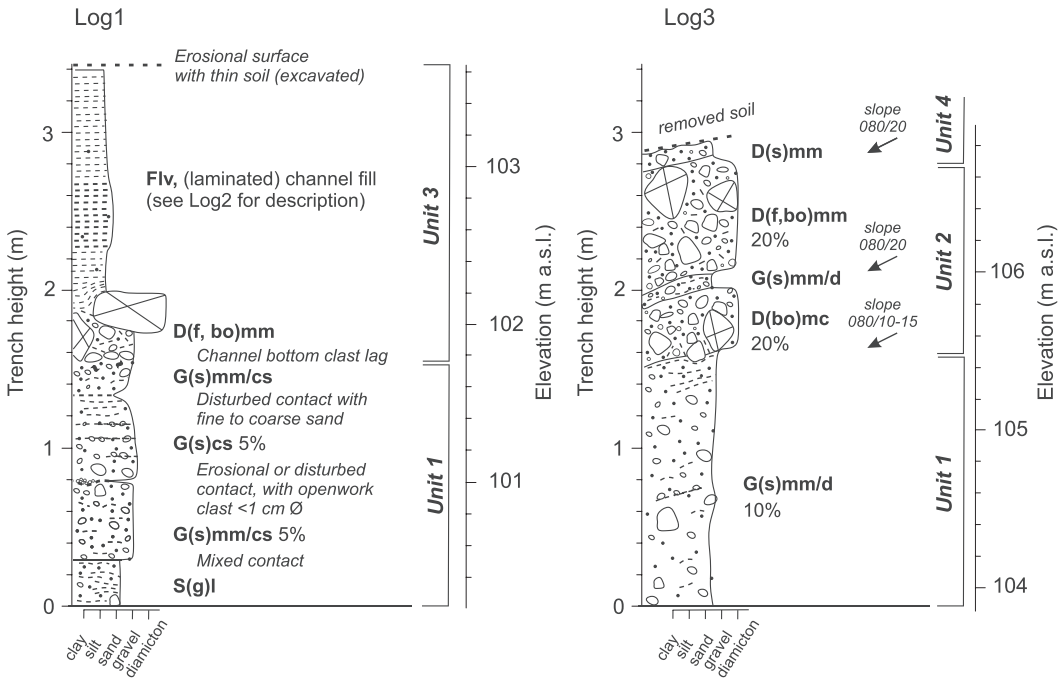

FIGURE 6 Lithofacies descriptions of Log1 and Log3 from the trench excavation TE1 (see Figure 4 for locations) with lithological units.

within fine-grained beds represent dropstones from the melting channel roof. Plastic deformation in the upper part of the fine-grained beds and laminae of Unit 3 is caused by the final melting of the glacier when the conduit roof collapsed and the deposition of Unit 4 took place.

The uppermost Unit 4 in field sections TE1 and TE2, which is composed of loose, poorly sorted, sandy, massive, and matrix-supported diamicton [D(s)mm] with a mixed lower contact, forms the topmost facies of the escarpment (Figures 4 and 6, Table 2). Unit 4 also forms the forest bed with podzol soil development. The diamicton is 0.2–1.0 m thick and its bottom is slightly fissile within the uppermost level of the escarpment. The unit becomes sandier, more mixed, and thicker along the slope of the escarpment. It also exhibits significant mass-flow deposition across the escarpment (Figure 4), as indicated by a channelized appearance towards the valley (LiDAR DEMs) and the appearance of boulder lags at the terrain surfaces (Figures 2 and 3). This is supported by the lithofacies geometry in the lower trench TE2, which reveals a clear channelization of Unit 4 with massive/matrix-supported diamicton about 7 m wide and 1 m thick, mostly containing pebbles and cobbles and lying over a channel fill of sediments of Unit 3 (Figures 4b and 5b).

Unit 4 is interpreted as flow till from flow of supra- and englacial material during the final melting of the ice sheet. In addition to stratigraphic position, two particular features of Unit 4 are proposed as diagnostic for flow till: (i) poor consolidation with unsorted particle size distribution, occasional boulders, and slight basal foliation; and (ii) significant flow characteristics with evidence of individual flow packages towards the valley (Bennett & Glasser, 2009). Unit 4 deforms the uppermost section of rhythmic laminations (Unit 3) with gravitational loading structures, and has thus been deposited later. The surface of Unit 4 was subsequently eroded by localized low-channel flows following the melting of the ice and the formation of surficial boulder lags, and was probably exposed to shoreline processes during the Yoldia Sea phase.

4.3 | Lithofacies of the fine-grained successions MJ1

The MJ1 section on the Lanajoki River Valley floor contains lithofacies association and characteristics (Unit 5) described in Figure 7 and Table 3. The lowermost Sub-unit 5a is composed of varves that consist of two laminae, a light-coloured melting season lamina and an overlying dark-coloured winter lamina composed of clay. Altogether, there are about 40 couplets of clay varves in this sub-unit. Sub-unit 5b is composed of massive clay with stable LOI (around 2%) and magnetic susceptibility decreasing upwards from 25 to 10 SI $\times$ 10^{-5} in the sub-unit. A sharp decrease of magnetic susceptibility is seen at the Sub-unit 5b/5c boundary, with subsequently upwards increasing LOI through Sub-units 5c, 5d, and 5e. Sub-units 5c and 5d are composed of massive clay gyttja and gyttja, respectively. They are superimposed by peat deposits (*Carex*, Sub-unit 5e) and massive agricultural sediments (Sub-unit 5f).

Unit 5 is interpreted to represent a lithofacies association that is typical for fine-grained (clayey) sediment succession in southern Finland, particularly for a location that was subaquatic during and after deglaciation, and has subsequently been isolated from the BSB (e.g. Pajunen, 2004; Virtasalo et al., 2014; Winterhalter, 1992). Glacial clay varves (Sub-unit 5a) are considered as classical glaciolacustrine clay varves deposited in front of the retreating glacier (e.g. De Geer, 1912), which were deposited in the proglacial lake of the BSB in the Yoldia Sea phase due to seasonal changes in meltwater discharge and the delivery of fine-grained silt and clay into the basin. At the time of their deposition, the highest shoreline was at about 155 m a.s.l. in the Murtoo village area, but rapidly regressed (3 m per 100 years) during the first millennia after deglaciation (Ojala et al., 2005). Sub-unit 5b is interpreted as a distal Ancylus Lake basin when the FIS had retreated further to the NNW and the relative sea level in the study area had dropped by 20–40 m. The isolation is well documented by a decrease in magnetic susceptibility and a transition to increasing LOI in the MJ1 sequence (Figure 7), which dates to the Ancylus Lake

TABLE 1 Lithofacies codes and their descriptions determined from section Log1. The interpreted units and their geometry in trench excavations TE1 and TE2 are presented in Figures 4 and 6

Unit	Lithofacies with description
3b–f	**Flv**: silt and clay laminations 1–3 mm thick. First coarsening up followed by upwards-fining silt laminations thinner with internal lamination 0.1–1 mm thick. Sharp contacts. Clay laminations thicker, weak internal lamination. Laminations conformable with over-large boulders. In the middle part laminations get thicker (0.5–2 cm). Occasional small dropstones 1–2 cm in size. Upper laminations more clayey with weaker laminations.
3a	**D(f,bo)mm**: diamicton with mixed and deformed clayey sand with outsized clasts and large boulders. Clasts subangular to subrounded.
1d	**G(s)mm/cs**: massive matrix-supported to crudely stratified sandy gravel. Coarsening up with silt/clay rafts of 1–2 cm and stratified/laminated and disturbed sand. Topmost part with 3 cm of weakly laminated/disturbed fine sand. Matrix is fine to medium sand. Mostly pebble–cobble gravel with occasional small boulders. Clasts are subangular to subrounded.
1c	**G(s)cs**: crudely stratified sandy gravel (weak clast layers) with local fining up to weakly stratified/laminated and disturbed sand. Topmost part with 3 cm-thick weakly laminated/disturbed fine sand. Matrix is fine to medium sand with mostly pebble–cobble gravel and occasional small boulders. Clasts are subangular to subrounded.
1b	**G(s)mm/cs**: massive, matrix-supported or crudely stratified sandy gravel. Poorly preserved, disturbed rhythmic sand beds/laminae, more gravelly with mostly pebbles to small cobbles and occasional large cobbles/small boulders. Overlain by poorly preserved silty fine sand with clay rafts 1–2 cm. Clasts are subangular to subrounded.
1a	**S(g)l**: remnants of rhythmic sand beds/laminae <2 cm thick in gravelly sand. Massive to weakly laminated fine to medium sand. Slightly disturbed with (silty) very fine to fine sand beds <1 cm thick. Spotted by granules and small pebbles. Clasts are subangular to subrounded.

TABLE 2 Lithofacies codes and their descriptions determined from section Log3. The interpreted units and their geometry in trench excavations TE1 and TE2 are presented in Figures 5 and 7

Unit	Lithofacies with description
4	**D(s)mm**: massive matrix-supported sandy diamicton. Loose and composed of coarse sand. Very poorly sorted with clayey matrix and occasional boulders. Mixed lower contact. Bottom section is slightly foliated and more clayey in the upper western part. Becomes mostly eroded towards the downslope. Yellowish brown and podzol soil with roots.
2	**D(f,bo)mm**: massive, matrix-supported diamicton. Matrix is clayey to fine sand. Very poorly sorted with frequent pebbles and some deformed sandy patches. Stone-% = 20–35%, the largest boulders up to 1.0 m Ø at a higher level of the unit and towards the western sector. Disc-shaped cobbles and boulders appear along the lower contact. Slightly compacted, hard to dig with excavator. Clasts are angular to subangular.
1	**G(s)mm/d**: massive, matrix-supported/deformed sandy gravel. Poorly sorted. Matrix from silty fine sand to very coarse sand. Contains poorly preserved sand beds except for the uppermost 20 cm that shows disturbed fine sand and medium-grained sand laminations 0.5–1.0 cm thick. Upper contact is mixed with cobbles and small boulders pressed into sand. Mostly pebbly with occasional large cobbles and small boulders. Stone-% = 10%. Clasts are subangular to subrounded.
2	**D (bo)mc**: massive, matrix- to clast-supported diamicton. Disturbed/mixed lower contact. Matrix mainly from clayey/silty fine sand to medium sand. Mainly cobbly with largest clasts of 0.4–0.5 m Ø. Stone-% = 20%. Clasts are angular to subangular.
1	**G(s)mm/d**: massive, matrix-supported/deformed sandy gravel. Poorly sorted. Matrix from silty fine sand to very coarse sand. Contains poorly preserved sand beds except for the uppermost 20 cm that shows disturbed fine sand and medium-grained sand laminations 0.5–1.0 cm thick. Upper contact is mixed with cobbles and small boulders pressed into sand. Mostly pebbly with occasional large cobbles and small boulders. Stone-% = 10%. Clasts are subangular to subrounded.

phase at 9.5 cal ka BP (Ojala et al., 2005). This was followed by a slow but steady increase in the organic matter content, representing the time when the Lanajoki River Valley floor was a larger isolated lake, the current Lake Murtoo being part of the basin (Sub-units 5c and 5d). Eventually, the larger basin was infilled by sediments and transformed into a peat bog (Sub-unit 5e) until anthropogenic land use (Unit 5f), while the deepest and most distal depression of the valley remained as a lake (the current Lake Murtoo). A hard bottom, probably composed of diamicton, was met at a depth of 1240 cm below the surface at the MJ1 coring location.

4.4 | Lithofacies of the fine-grained successions Log2

The section Log2 (Figure 8) is an example of the sediment composition and characteristics of fine-grained channel fill sediments (Unit 3) found in the TE1 and TE2 trench excavations (Figure 2). Field mapping with hand-driven probing and ground-penetrating radar profiles indicated that these channels continue uninterruptedly for hundreds of metres underneath each MRE and parallel to the Lanajoki River Valley, thus forming a widespread and branching network. Channels filled with fine-grained sediments are typically 5–10 m wide and 1–3 m thick at their thickest central part (Figures 4 and 5a and b).

The lithofacies association (Unit 3) in the Log2 sequence was divided into six sub-units (Figure 8, Table 4). The fine-grained Sub-units 3b–3f constituting the main part of the Log2 section are underlain by a sandy to bouldery channel base (Sub-unit 3a) and overlain by loose diamicton with flow characteristics (Unit 4). The division of the fine-grained lithofacies into sub-units was done because their thickness and the internal structure of 'laminae and bed couplets' vary considerably with depth (Figure 8). Sub-units 3b, 3e, and 3f are composed of a simple twofold structure (clayey part and silty part), whereas Sub-units 3c and 3d exhibit multiple (5–15) graded silt beds within each 1–7 cm-thick succession (Figure 9). Grain-size analysis of these laminae indicated that pale laminae systematically have a somewhat lower mean grain size than dark laminae, and that the silt

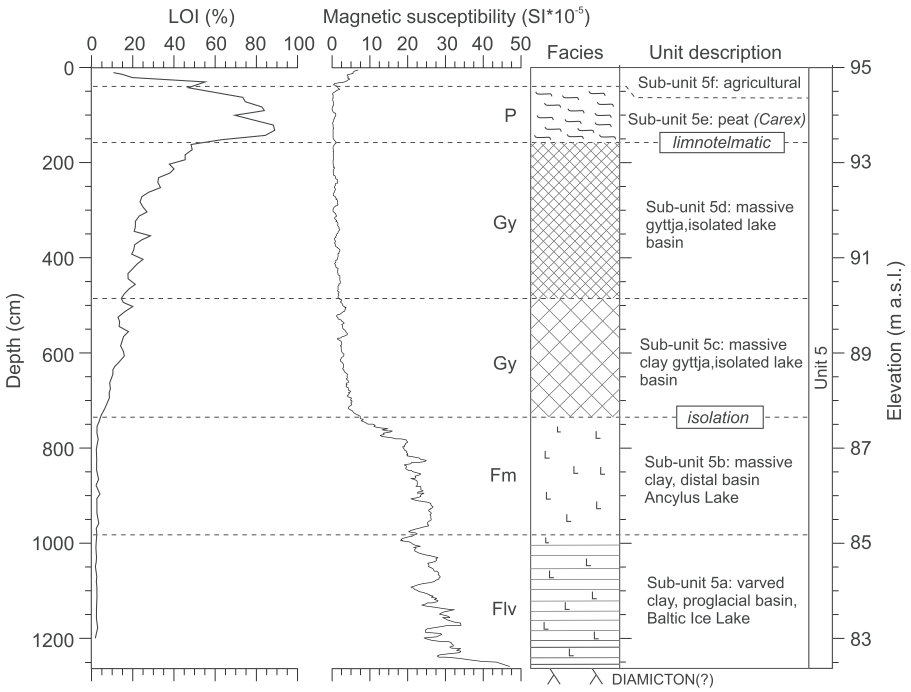

FIGURE 7 Physical characteristics and lithofacies descriptions of Unit 5 in the MJ1 core taken from the Lanajoki River valley floor about 300 m S–SW of Lake Murtoo.

TABLE 3 Lithofacies descriptions and interpretation of Unit 5 and sub-units in the MJ1 core presented in Figure 7

Unit	Troels–Smith coding	Lithofacies with description	Interpretation
5f	nig. 2, strafc. 0, elas. 0, sic. 0colour: light brown (5YR 5/4)struct: massivecomp: As 1, Ag 1, Gmin 1, Tb 1	**Agricultural layer**: massive, composed of clay and lenses of sand, signs of ploughing and harvesting	Land use layer, agricultural purposes, currently as fallow land
5e	nig. 3, strafc. 0, humo 1, lim. 0colour: brown (5YR 5/2)struct: massivecomp: Tb 4, Tl+	**P** (peat): homogenous peat (*Carex*) composed of partly decomposed plants and particles and water horsetail	A peat bog formed by filling of a lake basin with plant debris after isolation
5d	nig. 3, strafc. 0, elas. 1, sic. 1, lim. 0colour: dark brown (5YR 2.5/1)struct: massivecomp: Ld 4, Dl+, Dh+	**Gy** (gyttja): homogenous fine detritus material with occasional pieces of coarser detritus and plan material	A smaller lacustrine basin or a calm bay of a larger lake. Sediments mostly derived from autochthonous primary production
5c	nig. 2, strafc. 0, elas. 1, sic. 1, lim. 0colour: dark brown (5YR 2.5/2)struct: massivecomp: Ld3, As 1	**Gy** (clay gyttja): homogenous fine detritus material with occasional clayey and silty sections, no detectable interbedded laminae	A larger lacustrine basin following the isolation from the Baltic Sea basin. Mineral matter erosion from the catchment and autochthonous primary production
5b	nig. 1, strafc. 1, elas. 0, sic. 2, lim. 1colour: grey (5YR 3/1)struct: massivecomp: As 4	**Fm** (clay): homogenous clay with occasional sulphidic grains and layers of coarser mineral material	Distal lake basin (Ancylus Lake) of the Baltic Sea, ice margin retreated further to the NW. Deposition of mineral matter with ever-increasing autochthonous production
5a	nig. 1, strafc. 4, elas. 0, sic. 2, lim. 0colour: grey (5YR 5/1)struct: laminated (varved) comp: As 4, Ag+	**Flv** (varved clay): distinctive and regular rhythmites with clay and silt laminae, normal grading is observed within laminae couplets	Proglacial lake basin in front of the retreating glacier (Yoldia Sea phase). Seasonal variation in mineral matter deposition and grain size due to glacier melting at the ice margin

content of these sediments varies between 10 and 50% (see Supplementary Data S3). We note that this grain-size data are converse to the classic proglacial clay varve, in which the light layer usually comprises a coarser lamina set (De Geer, 1912; Zolitschka et al., 2015). This is because dark laminae contain a larger proportion of biotite flakes than pale silty laminae, suggesting a local source from biotite-rich bedrock, thus causing a darker tone. Biotite flakes have lower settling velocity than silicate minerals of quartz and feldspars (e.g. Garzanti et al., 2008). Additionally, the silt content of Sub-units 3b–3f is higher in samples taken from the bottom part of the channel fill section, which indicates an upwards-fining sequence of Unit 3.

The important common and shared characteristics of Sub-units 3b–3f are that they all exhibit bed-parallel laminae and show draped channel fill bedding without any disturbance, such as faults, folds, or contorted structures. The laminae are composed of clay and silt-sized fractions of mineral matter without a significant amount of organic matter (Figure 8, Supplementary Data S2 and S3). The general plunge (5–10°) of laminae is parallel with the direction of the channels. The

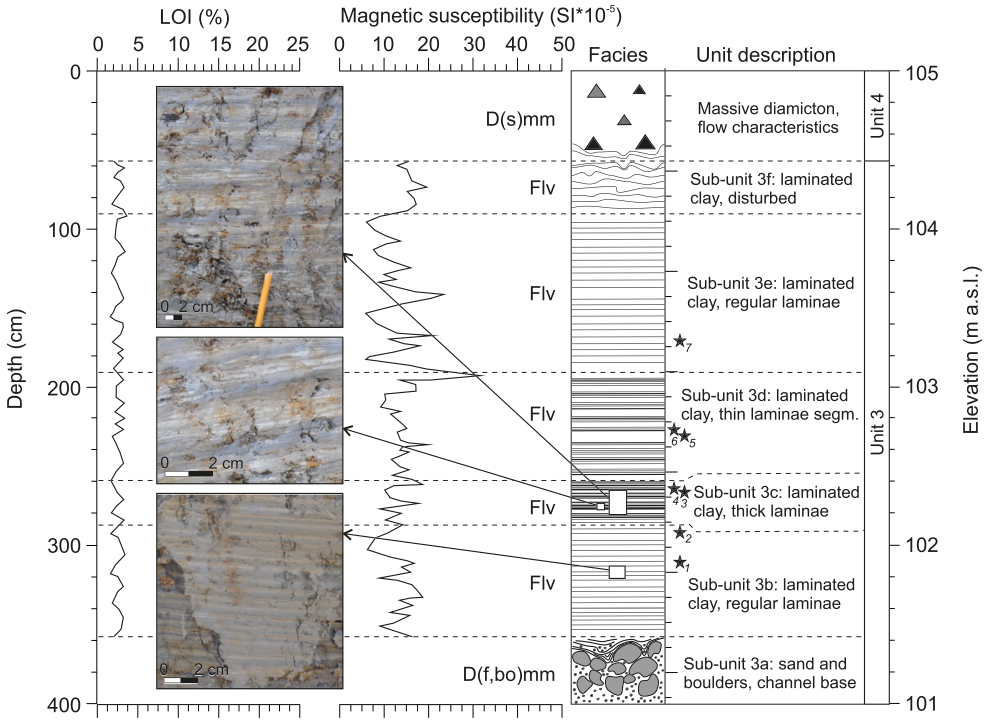

FIGURE 8 Physical characteristics and lithofacies descriptions of Units 3 and 4 in section Log2 conducted from an excavated trench wall shown in Figures 5a–d. Samples for grain-size analysis (see Supplementary Data S1 and S2) have been marked with black stars.

TABLE 4 Lithofacies descriptions and interpretation of Units 3 and 4 in section Log2 presented in Figure 8

Unit	Troels–Smith coding	Lithofacies with description	Interpretation
4	nig. 1, strafc. 1, elas. 0, sic. 0colour: greyish brown (5YR 4/4)struct: massivecomp: Gg (min.) 3, Gg (maj.) 1, Ag+	**D(s)mm**: sandy diamicton, massive or weak laminations, weak flow structures and poor sorting, poorly developed fabric, forest podzoil bed	Flow till (cover till) representing the final melting of the ice sheet. Disturbed by roots and forest bed activity
3f	nig. 1, strafc. 4, elas. 0, sic. 2, lim. 0colour: dark grey (5YR 4/1)struct: laminated, disturbedcomp: As 4, Ag+	**Flv**: disturbed clay and silt laminae	Subglacial channel fill, suspension fallout in weak water flow (traction), disturbed by diamicton mass flow deposit
3e	nig. 1, strafc. 4, elas. 0, sic. 2, lim. 0colour: dark grey (5YR 4/1)struct: laminatedcomp: As 4, Ag+	**Flv**: rhythmically laminated clay and silt couplets, occasional thicker silt laminae, altogether c. 30–40 laminae couplets	Subglacial channel fill, suspension fallout in weak water flow (traction) and with occasionally changing flow regimes and sediment delivery
3d	nig. 1, strafc. 4, elas. 0, sic. 2, lim. 0colour: dark grey (5YR 5/1)struct: thinly laminatedcomp: As 3, Ag1	**Flv**: rhythmically laminated clay with multiple (3–10) silt laminae within each 1–2 cm thick succession, altogether 25–30 successions	Subglacial channel fill, suspension fallout in weak water flow (traction) and with constantly changing flow regimes and sediment delivery
3c	nig. 1, strafc. 4, elas. 0, sic. 2, lim. 0colour: dark grey (5YR 5/1)struct: thickly laminatedcomp: As 3, Ag1	**Flv**: rhythmically laminated clay with multiple (10–15) silt laminae within each 4–7 cm thick succession, undulant surfaces, 4 successions	Subglacial channel fill, suspension fallout in weak water flow (traction) and with constantly changing flow regimes and sediment delivery
3b	nig. 1, strafc. 4, elas. 0, sic. 2, lim. 0colour: dark gray (5YR 4/1)struct: laminatedcomp: As 4, Ag+	**Flv**: rhythmically laminated clay and silt couplets, very regular in thickness (10–12 mm), altogether c. 50–60 laminae couplets	Subglacial channel fill, suspension fallout in weak water flow and high regime traction in shallow water
3a	nig. 1, strafc. 1, elas. 0, sic. 0, lim. 1colour: greyish brown (2.5Y 4/2)struct: massivecomp: Gg (maj.) 2, Gg (min.) 2	**D(f,bo)mm**: boulders up to 2 m in diameter, irregular sizes, interspaces filled with sand and overlain by fine-grained laminated sediments	Subglacial channel erosion, fast water flow in subglacial channel, truncated and discontinuous indicating significant channel base formation

plunge direction follows the terrain relief along the channels. Inclined internal bedding, such as cross-bedding and cross-lamination, as well as other microforms (e.g. ripples, climbing ripples), are absent from Sub-units 3b–3f. All contacts between Sub-units 3b–3f are gradational and no erosional unconformities can be detected. Laminae and bed couplets also lack sharp boundaries that are commonly observed in varved sediment between winter and summer layers (De Geer, 1912; Zolitschka et al., 2015). The laminated section (Sub-units 3b–3f) does not contain interbedded layers of coarser material (sand or granules) but contains occasional sand- to granule-sized dropstones within the fine-grained deposits. We counted 180–190 lamina couplets or successions from Sub-units 3b–3e, several tens of

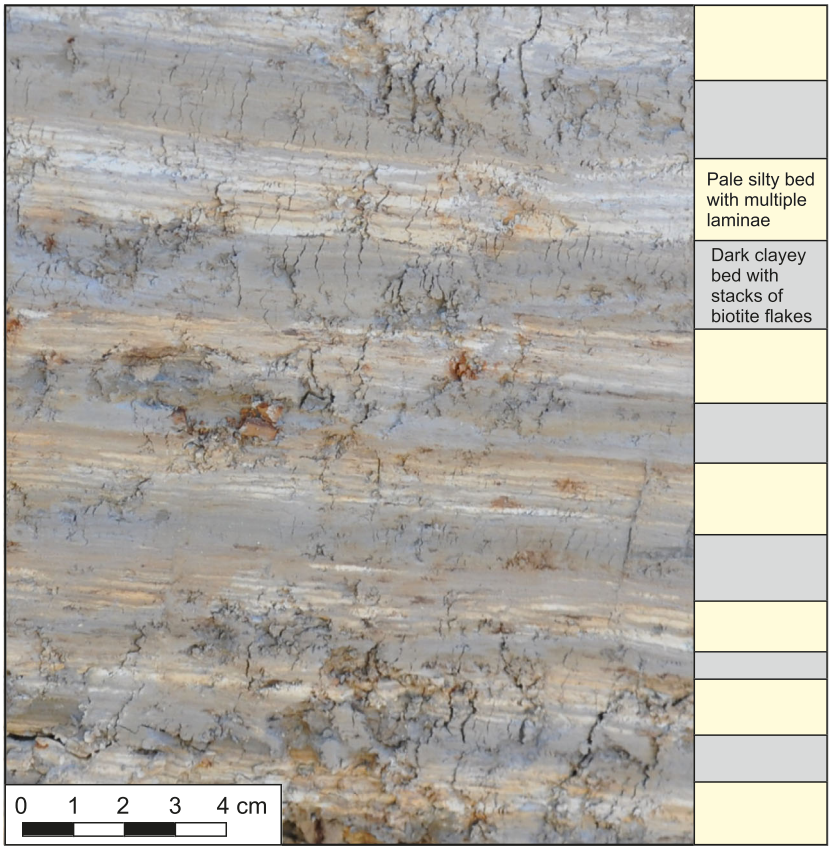

FIGURE 9 The middle part of the Log2 sequence (Sub-unit 3c, depth of 270 cm) exhibits undisturbed rhythmically deposited beds of silty laminae part and more clayey part, which were deposited in a subglacial meltwater channel.

couplets deposited in boulder interspaces (Sub-unit 3a), and several tens of contorted or disturbed uncountable couplets in the uppermost Sub-unit 3f. Altogether, it is estimated that Unit 3 contains 230–260 lamina couplets or successions.

Unit 3 is interpreted to represent deposition in subglacial channels, in association with the formation of MREs and the development of subglacial meltwater networks. The laminated pattern of channel fill deposit probably reveals subglacial ice-bed coupling/uncoupling by fluid pressure at the ice-bed interface with fluctuating rate of drainage and deposition processes (e.g. Bennett et al., 2006; Clerc et al., 2012). Although Unit 3 bears striking resemblance to proglacial lacustrine varved sediments, we noted several distinct differences that lead us to an alternative explanation. The most important evidence of subglacial origin is that finely laminated channel-fill sediments of Unit 3 are covered by 10–60 cm-thick massive diamicton (Unit 4), which has been interpreted as flow till related to the final melting of the ice sheet in the area. The uppermost part of Unit 3 indicates disturbance (loading structures) caused during the deposition of Unit 4 (Figures 8 and 9), indicating that it was deposited later than fine-grained sediments of Unit 3.

Further evidence is that the lithofacies characteristics, thickness, and a number of laminae/bed couplets in Sub-units 3b–3f are different from glacial varves found in the MJ1 section (Sub-unit 5a) and from those typically described in the BSB area (De Geer, 1912). Couplets in Sub-units 3b–3f do not have sharp boundaries and they are more complex, with multiple 'pulses' and silt deposition 'events' compared with classical clay varves. Also, scattered gravel and pebbly grains within undisturbed finely laminated clay and silt sequences (Sub-units 3b–3e) are interpreted to represent melt-out of debris from the subglacial channel roof during deposition. Finally, on the higher-lying edge of these channels, diamicton (Unit 2) has partially intruded into Unit 3, suggesting their synchronous formation (Figure 4). This may indicate minor ice sheet activation towards the valley during deglaciation, when channels were active and being filled by fine-grained sediments. It also indicates lack of over-pressurizing of sediments during and after their deposition, thus indicating disconnected periodic drainage, as discussed more thoroughly below (Bennett et al., 2006; Clerc et al., 2012).

5 | DISCUSSION

5.1 | Formation of MREs and the evolution between inefficient and efficient subglacial drainage

In this study, sediment descriptions (Figures 4–8) and regional geomorphology (Figure 2) lead to increased understanding of subglacial deposition in enlarged cavities and subglacial tunnels during the FIS deglaciation, with significant meltwater activity along subglacial meltwater routes. The results show that the formation of murtoos (TTMs and CTMs) in a transient, semi-distributed subglacial hydrological system triggered by meltwater drainage (Mäkinen et al., 2019; Ojala et al., 2021; Peterson Becher & Johnson, 2021) is interconnected with channelized drainage and the deposition of eskers via the MREs. In the following, we present the main phases of MRE formation (Figure 10), together with the evolution of subglacial drainage pathways (Figures 11 and 12) in the Lake Murtoo area.

In the first phase (Phase 1, Figure 11), fields of murtoos were formed when a significant amount of meltwater was delivered to the

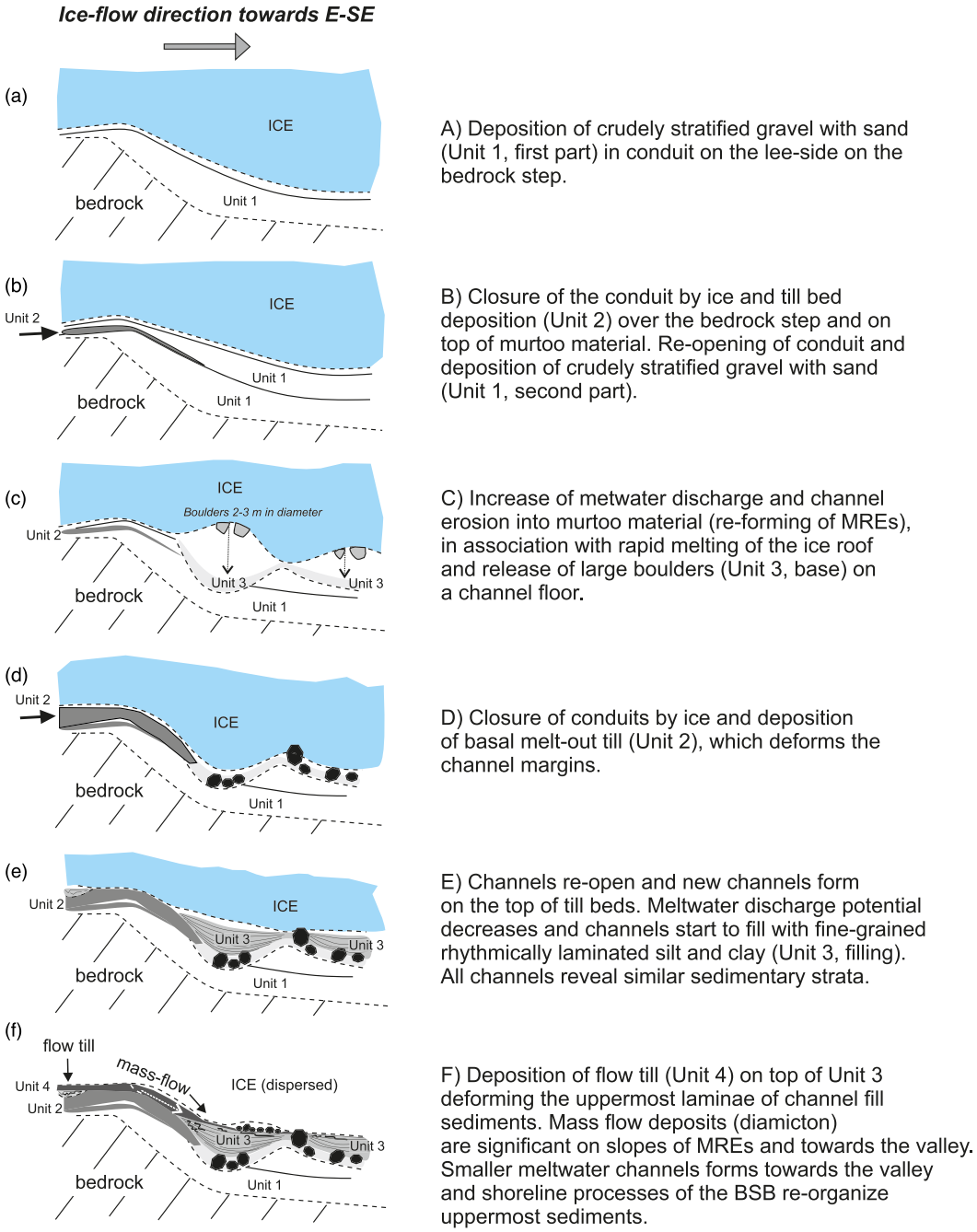

FIGURE 10 Schematic presentation of the formation of lithofacies associations (Units 1–4) across the MRE. The topographical environments and the main phases of sedimentation, deformation, and erosion across the MRE are summarized with lithofacies units given in Figures 4 and 6.

ice bed and enlarged subglacial conduits and cavities became filled with sandy diamicton under high-pressure conditions (Mäkinen et al., 2017, 2019). This phase represents the time when the ice margin was probably some 50–70 km SE of the Lake Murtoo area and the subglacial hydrology was characterized by semi-efficient drainage with an effective pressure fluctuating close to zero (Mäkinen et al., 2019; Ojala et al., 2019) (Figure 13). Deposition of crudely stratified gravel and sand (Unit 1, lower part) occurred in a conduit that was formed on the lee side of the bedrock step relative to the ice-flow direction (Figure 10a). It was followed by a closure of conduits and cavities, and then re-opening and deposition of an upper part of Unit 1 (Figure 10b), caused by ice-bed coupling and uncoupling episodes in response to hydrological forcing and ice creep at the bed (Bennett et al., 2006; Kamb, 1987). This type of sediment deposition, lithofacies, and structural characteristics of Unit 1 resemble those often described in murtoo bodies (Mäkinen et al., 2017, 2019), and we consider that this unit was deposited simultaneously and by similar subglacial processes with the formation of murtoos in the present study area (Figure 2).

Where apices of TTMs correlate strongly with local ice-flow direction and facies preferentially form beds that slope down-ice, the direction and facies beds of MREs in the Lanajoki River valley point towards the south (Figure 2). This probably indicates subglacial conduit development on the lee side of obstacles, where enlarged cavities are linked by connections that form a linked-cavity network (Bennett et al., 2006; Kamb, 1987). It could also be that increased ice-bed

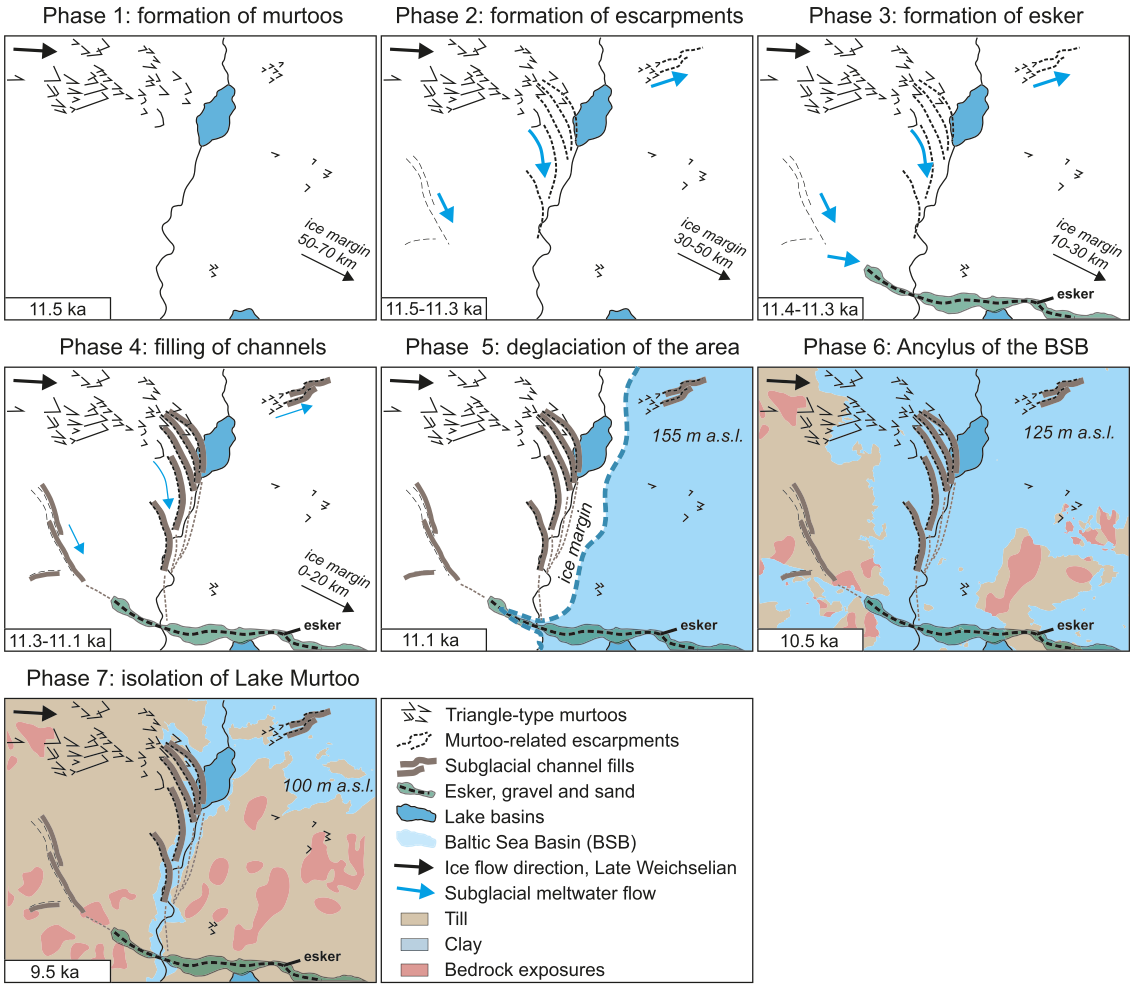

FIGURE 11 Evolution of the Lake Murtoo study area during deglaciation (between 11.5 and 9.5 ka BP). Different phases (1–7) represent successive and interrelated deposition/erosion processes associated with a transition between semi-distributed (phase 1) and channelized (phase 3) drainage with subglacial filling of meltwater channels (phases 4 and 5) and regional deglaciation and isolation (phases 5–7). The estimated distance to the ice margin is given for phases 1–4 and an elevation of the Baltic Sea shoreline (Ojala et al., 2013) for phases 5–7.

uncoupling due to fluid overpressure contributed to the enlargement of cavities and deposition of crudely stratified diamicton in transverse ridges that initially form the core of MREs (Unit 1) (Bennett et al., 2006; Clerc et al., 2012). These observations are in accordance with excavations into murtoo-related ridges and escarpments by Ojala et al. (2021), revealing that the main sediment characteristics of different murtoo types are similar, independent of their morphometric appearance. It adds to the discussion of equifinality of processes and landform that emerges in the subglacial environment (Menzies et al., 2018; Möller & Dowling, 2018).

In the second phase (Phase 2, Figure 11), the water arriving at the bed exceeds the subglacial drainage capacity, causing water pressure to build up and counteract with the weight of the glacier (Cuffey & Paterson, 2010). Increased water pressure shifts effective pressure away from the murtoo-forming environment, forcing the direction of TTMs NW of Lake Murtoo to turn towards the south-opening Lanajoki River Valley (Figure 2b). Terraces of the MREs appear immediately from the large murtoo field, representing the subglacial drainage direction of pressurized water. By that time, subglacial drainage became more arranged and modified slightly curved escarpments (MREs), creating terrace-like morphology along the margin of the valley (Figures 2 and 3). The transition from semi-distributed towards more connected drainage probably relates to increased meltwater delivery (higher water pressure), thus forcing larger drainage systems to develop quickly, concurrently with the approaching ice margin (Doyle et al., 2021; Lewington et al., 2020; Rada & Schoof, 2018) (Figure 11). Based on excavation, meltwater routing during this transition from low- to moderate-flow subglacial environment (Clerc et al., 2012) was guided by the underlying bedrock topography, along which subglacial meltwater was collected and evacuated towards the southern part of the Lanajoki River Valley. This process caused considerable erosion of the underlying terrain (Unit 1) and created meltwater channels alongside MREs (Figure 10c). The channels are evidence of the spatial evolution of the drainage to develop towards a more efficient meltwater flow environment. As a consequence, the base of Unit 3 was formed in association with melting of the ice roof and releasing large boulders on a channel floor.

Concurrently with the formation of MREs and related channels, the ice flow from the west deposited basal melt-out till (Unit 2, Figures 4–6) over the escarpment, while simultaneously trying to close the conduits and deform their margins (Figure 10d). This process is evidenced by till beds that are intercalated with gravel beds, indicating continued conduit flow between till-depositing ice-flow events restricting the conduit size and formation of subglacial channels.

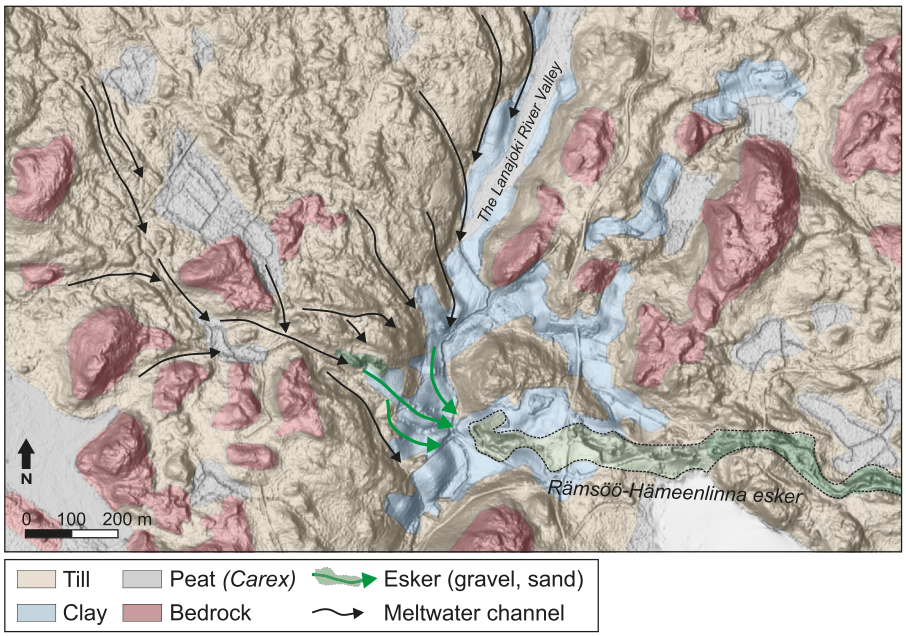

FIGURE 12 Subglacial drainage routes in the southern part of the Lanajoki River valley, where meltwater channels associated with MREs (from the north) and narrow parallel ridges (from the west) meet the onset of the Rämsöö–Hämeenlinna esker.

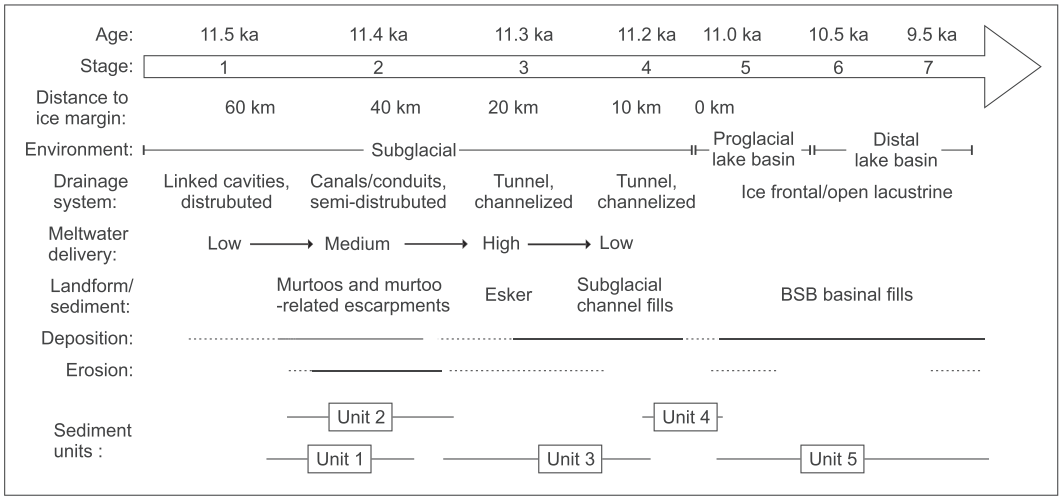

FIGURE 13 Schematic diagram depicting the distance to the ice margin with the deglaciation chronology for the Lake Murtoo study site (see Figures 10 and 11). The development from a subglacial to a proglacial sedimentary environment is associated with significant changes in the drainage characteristics and depositional/erosional phases. The described lithofacies-based Units 1–5 are placed in the diagram

In the third phase (Phase 3, Figure 11), the more connected subglacial hydrology led to channelized efficient drainage when the ice margin approached the Lake Murtoo study area and tunnels could be formed. Large boulders at the bottom of subglacial channels (Sub-unit 3a) indicate rapid expansion of conduit roofs and mixing of boulders with channel bottom gravel and sands in a high-flow meltwater environment. This drainage system expansion to channelized efficient drainage was associated with the formation of the Rämsöö–Hameenlinna esker, which strictly begins from the southern part of the Lanajoki River Valley (Figure 12). Moreover, the terrain characteristics indicate that the Lanajoki River Valley route is not the only subglacial drainage route that leads to this esker; there are also several meltwater sources from the west that fed the tunnellized flow (Figure 12). These routes have characteristics of murtoos and MREs, although morphologically somewhat less distinct compared with the main route. Taken together, we suggest that MREs' murtoo-like forms were eventually deformed and guided hydrological routing along which subglacial meltwater was evacuated towards the R-channels (Boulton & Hindmarsh, 1987; Ojala et al., 2021; Röthlisberger, 1972).

In the fourth phase (Phase 4, Figure 11), meltwater routes were disconnected from the main regional subglacial hydrological system, but the remaining uncollapsed channels were still periodically used as low-flow tributaries that evacuated meltwater towards the ice margin. These channels were filled with an undisturbed set of thinly laminated clay and silt sediments (Sub-units 3b–3f), until reaching the ice-marginal environment and the final melting of the FIS in the area (Figure 10e). Rhythmically laminated channel fills indicate laminar subglacial water flow, possibly due to diurnal and/or seasonal spilling over of the reorganized subglacial hydrological system. These sediments are overlain by Unit 4, which was deposited as flow till, as evidenced by the loose composition, slight basal foliation, and loaded deformation of laminations in the upper part of Unit 3 (Figure 10f). The slope

of the escarpment is associated with flow characteristics of diamicton, as indicated by the downstream channelization of Unit 4 towards the valley.

Finally, the Lake Murtoo study area was exposed underneath the ice sheet at around 11.1 ka (Phase 5, Figure 11) and isolated from the BSB at around 9.5 ka BP (Phase 7, Figure 11), exposing it to shoreline processes, forest bed and podzol soil development, and frost heave activity. Proglacial varved sediment and postglacial gyttja and peat (Figure 7, Sub-units 5a–5e) were deposited in the Lanajoki River Valley during phases 6 and 7 and the following millennia. These sediments only cover the valley floor up to an elevation of about 100 m a.s.l.

5.2 | Deposition of fine-grained laminated sequence in subglacial channels

Filling of channels alongside MREs with the thinly laminated silt and clay sediments of Unit 3 indicates sedimentation in a suspension-load-dominated environment in shallow subglacial channels with relatively low, but repetitiously changing, flow velocities (e.g. Bennett et al., 2006; Hodder & Gilbert, 2007). The development of such a depositional environment probably relates to three interrelated reasons: the drainage was disconnected from the main subglacial drainage route, which transferred to another location; the overall flow of ice was simultaneously decreased or terminated, leaving uncollapsed channels; and these channels were used for repeated lower-magnitude drainage that periodically flooded the abandoned drainage system, possibly slightly expanding the channels and filling them with fine-grained sediments. The display of fine-grained sediments, as well as the relatively low appearance of only sand- to granule-sized dropstones within them (Unit 3), clearly associates with a shallow subglacial channel environment with generally low flow velocities. Under these circumstances, the melting of the channel ice roof and passive release of debris as rain-out is periodic and minor (Bennett et al., 2006). The lack of deformation of Unit 3 is consistent with a shallow sub-glacial settling depth from laminar flow, controlled by the channel height (Clerc et al., 2012).

The sharp onset of laminated silt/clay deposition on top of Sub-unit 3a in the Log2 sequence supports the interpretation of rapid transition from high- to low-flow environment, probably indicating that these channels were abruptly disconnected from the main meltwater drainage routes and functioned as small tributaries with water that was essentially standing and periodically moving very slowly. It has been documented with valley glaciers that a transition from connected to disconnected subglacial drainage can happen abruptly, but the environment is often associated with disconnection and reconnection 'events' because of water pressure changes in the up-ice direction (Rada & Schoof, 2018). Moreover, the absence of laminae disturbances, erosional characteristics, and layers of coarser (sand) material in Sub-units 3b–3f indicates an absence of water turbulence during the deposition of fine-grained sediment, and suggests that there was no major increase in water flow energy or change in flow direction in these channels once the deposition of fine-grained laminae initiated. Although the settling velocity for silt- and clay-sized particles is generally $<1\ cm\ s^{-1}$, it is difficult to estimate the exact magnitude of water flow velocity in these channels, especially because recent studies have shown that flocculation into larger aggregations is significant in subglacial settings and sediment-concentrated water, and settling velocities can thus be greater than the diameters of individual grains would suggest (Hodder & Gilbert, 2007).

Architectural and sedimentological characteristics of subglacial laminated sediments presently depicted from the Lake Murtoo sections (Sub-units 3b–3e) have seldom been described. They resemble those sometimes found in subglacial lakes that drain meltwater from the ice-sheet interior to its margin via meltwater networks (Kuhn et al., 2017). Lesemann et al. (2010, 2011) described a subglacial sequence up to several tens of centimetres thick, composed of as many as 40 alternating silty and clayey couplets in the Island of Funen, Denmark. They interpreted that these sediments were deposited in subglacial cavities and in slack water conditions during intervening quiescent conditions when glacier coupling had regionally decreased and subglacial cavities were able to develop. They represent similar rhythmic sedimentation to Sub-units 3b–3f in the present study, however, fine-grained laminated sediments in the Lake Murtoo area are found in channels and do not exhibit ductile deformation, thus probably representing deposition in the disconnected drainage systems closer to the ice margin.

Christoffersen et al. (2008) described a thick fine-grained sedimentary section in the Christie Bay area deposited in a subglacial lake beneath the LIS. They interpreted basin fill in a dynamic subglacial lake environment where sediments and beds of variable grain sizes were delivered by discharge of meltwater from a larger subglacial water system. Munro-Stasiuk (2003) described a subglacial glaciolacustrine sequence of Lake McGregor, which has many similarities with Unit 3 described in the Log2 section in the Lake Murtoo area. In particular, silty to clay couplets that often exhibit multiple silty laminae in each succession. The significant difference between Unit 3 and that described by Munro-Stasiuk (2003) is that the Lake McGregor section contains diamicton interlayers that disturb fine-grained laminae structure, thus representing ice-flow activity and gravity flow events in a more chaotic deposition environment. Munro-Stasiuk (2003) interpreted that sedimentation indicates changes in interconnected cavity systems where water accumulation and drainage events played a key role along the main routes of water flow beneath the LIS.

Livingstone et al. (2015) consider difficulties in discriminating between proglacial and subglacial sediments. They conclude that the style of sedimentation and deformation is an efficient way of separating deposits of these two environments where subglacial sediments deposited under ice-bed decoupling periods may be better preserved due, for example, to passive sedimentation and fluidization and hydrofracturing within discrete water-lubricated sediment packages. As such, Clerc et al. (2012) documented stratified sand and gravel deposition in subglacial cavities where ice-bed uncoupling and subglacial cavitation provided available space for sedimentation under the British–Irish Ice Sheet. Although their sediments were generally composed of coarser material than in the Log2 sequence, the channelized appearance is very similar in shape and size to subglacial channels in the Lake Murtoo study area. Also deposited underneath the British–Irish Ice Sheet, Ravier et al. (2014) described sections of laminated fine-grained sediments within diamicton and gravelly facies. Interestingly, clay layers exhibit numerous granule- to cobble-sized clasts, analogous to what we see in Sub-units 3b–3e facies in the Log2

sequence. They interpret that laminated fine-grained sediments were deposited by settling of finer suspended particles during quiescent phases of subglacial drainage.

5.3 | Evidence from subglacial water pressure fluctuations

The distinct rhythmic deposition of laminae in subglacial channels in the Lake Murtoo Log2 sequence (Sub-units 3b–3e) is interpreted as associated with periodic changes in the sediment suspension load and water flow velocity. The commonly recognized periodic changes in subglacial drainage result from diurnal and seasonal fluctuations, with generally the largest amount of meltwater delivered to the glacier bed during summer (e.g. Chu et al., 2016; Sundal et al., 2011). Moreover, as subglacial channels are often fed from a mixture of subglacial, englacial, and supraglacial sources, the pulsatory nature of laminated fine-grained fill sediments may indicate cyclical changes in the evolving subglacial drainage in response to changes in glacial meltwater sources, glacier geometry, and/or flow dynamics, and recharging and drainage of water in subglacial cavities and potential lakes up-ice (Nienow et al., 2017). It is known, for example, that even relatively small (10%) changes in seasonal subglacial water pressure can significantly modify water flow paths (Chu et al., 2016) and thus force the patterns of temporal variability and spatial distribution in water flow (energy) across hundreds of kilometres.

Doyle et al. (2021) documents water pressure pulses underneath the Greenland ice sheet during melting, which they suggest provides evidence for gap opening and closing at the ice–sediment interface in response to changes in water pressure. There is also evidence that when surface melting ceases, the upstream and downstream ends of these channels may freeze shut, thereby trapping water at the glacier bed (Copland et al., 2003; Skidmore & Sharp, 1999). These changes associated with opening and closure of subglacial channels, or/and episodic discharge of supraglacial or subglacial water masses (Clerc et al., 2012), probably explain the deposition of the clayey to silty laminae sequences in MRE-related channels in the Murtoo study area.

If surface melting provides a significant input to subglacial drainage, water flux and energy tend to have strong seasonal characteristics with very different configurations in summer and winter. Moreover, subglacial drainage in ice sheet areas that are subjected to strong surface melting are accompanied by significant changes in daily runoff amplitude and diurnal variation in runoff and water pressure that are cyclic in areas close to channels (Gordon et al., 1998; Willis et al., 2003). The presently described channel-fill sediments potentially reflect both of these periodic characteristics in their complicated lamina successions in Sub-units 3b–3f. If the deposition of 230–260 lamina couplets of Unit 3 reflects an annual cycle of sedimentation, the subglacial meltwater channels must have remained uncollapsed and in constant use for slow subglacial drainage for about 25 km (c. 250 years) of ice margin retreat, with ice recession rates of about 100 m a^{-1} reported by Sauramo (1923). This is possible according to our regional evolution model only if the channels were active through phases 3 and 4 (Figure 11). This cannot be excluded, considering that Chandler et al. (2021) recently showed from Greenland that a fast/efficient subglacial drainage system can develop beneath >900 m-thick ice, extend ~50 km from the ice margin, and persist with little response to meltwater inputs via moulins. However, we consider annual cyclicity as an unlikely scenario, because of the complexity of subglacial processes during deglaciation (e.g. Bennett & Glasser, 2009) and because of the complex characteristics of the laminae/bed set in the sequence (Unit 3). We find it a more plausible explanation that laminated sequences in Log2 and other subglacial channels along Te1 (Figure 4) represent more frequent and variable changes of subglacial hydrology than annual cyclicity. Most likely, a combination of diurnal changes in runoff (silt layers) and sub-seasonal melt 'events' in subglacial hydrology.

Increased melting and an elevated subglacial water pressure also reduce the contact between the ice and the terrain surface, causing increased ice-flow velocity (Bartholomew et al., 2010; Iken & Bindschadler, 1986). As the ice continues to slide at some distance in the up-ice direction, the subglacial drainage closer to the margin experiences pulses of meltwater that are directed to the already existing subglacial meltwater channels and disconnected spill-over routes that have not collapsed. It has been documented that subglacial water pressure variations in disconnected areas can occur due to bridging effects of drainage systems and potentially due to ice motion (Davison et al., 2019), which can cause low-amplitude and high-frequency pressure variations, even in distant locations (Chu et al., 2016; Rada & Schoof, 2018).

Furthermore, Mejia et al. (2021) provided a conceptual model of diurnal subglacial floodwaves triggered by rapid lake drainage events. These events caused expansion of isolated cavities where floodwaters connected adjacent linked cavities and previously isolated or weakly connected cavities by driving meltwater laterally into the distributed system. The rhythmic nature of sedimentation in the presently described subglacial channels (Sub-units 3b–3f) could relate to such pressure variations and switching between inefficient (cavities) and efficient (channelized) drainage in the up-ice direction, thus indicating the volume of meltwater generated up-ice and the growth of channels or branching of new areas at the glacier bed (Fenn et al., 1985). There is also evidence from Greenland and Antarctica that large and periodic changes in subglacial hydrology can be driven by sudden drainages of supraglacial lakes or repeated filling and drainage cycles of subglacial lakes, causing brief pulses of meltwater delivery to the ice sheet bed (e.g. Das et al., 2008; Fricker et al., 2007; Malczyk et al., 2020). The potential appearance of a subglacial lake in the Lake Kulovesi basin during deglaciation could explain the rhythmic sedimentation in subglacial channels (Sub-units 3b–3f) in the Lanajoki River Valley as a consequence of repeated filling and drainage cycles in lake hydrology (e.g. Das et al., 2008; Fricker et al., 2007; Malczyk et al., 2020). However, the Lake Murtoo area is so distant from subglacial lakes that drainage events and higher discharge does not lead to deposition of sand- or gravel-size layers in these channels. We consider that one of the processes described above, or a combination of these processes, has driven the hydrological cyclicity and sedimentation of the fine-grained laminated sequence in the presently studied subglacial channels (Sub-units 3b–3f).

6 | CONCLUSIONS

This paper presents geomorphological and sedimentological evidence for the evolution of subglacial drainage pathways beneath the retreating FIS during the Weichselian deglaciation. Results from the Lake Murtoo area (SW Finland) reveal a widespread and dynamic subglacial

drainage system connecting weakly effective semi-distributed (murtoos) to effective tunnellized (esker) water flow via erosional MREs. In accordance with previous studies, the presented evidence suggests that a key control on the formation of murtoos and MREs is the meltwater input and efficiency of the subglacial drainage system, which are associated with ice-flow dynamics. Moreover, this paper documents the lithofacies architecture of flow till-buried fine-grained sediments that were subglacially deposited in disconnected erosional drainage channels. The appearance of rhythmically laminated silt and clay sediments in these channels indicates sedimentation in a suspension-load-dominated environment in a shallow subglacial channel with relatively low, but repetitiously changing, water flow velocities, probably reflecting periodic spill-over events in isolated tributaries due to diurnal and/or seasonal water pressure changes in the up-ice direction.

ACKNOWLEDGEMENTS

We are grateful to two anonymous reviewers for their constructive suggestions and comments. This work was supported by the Academy of Finland (Grant No. 322252 to Antti E.K. Ojala and Grant No. 322243 to Joni Mäkinen).

CONFLICT OF INTEREST

The authors have no conflict of interest to declare.

DATA AVAILABILITY STATEMENT

Data supporting the results of this work are available on request from the authors.

ORCID

Antti E. K. Ojala https://orcid.org/0000-0001-8272-4835
Joni Mäkinen https://orcid.org/0000-0002-3613-7418

REFERENCES

Ahokangas, E., Ojala, A.E.K., Tuunainen, A., Valkama, M., Palmu, J.-P., Kajuutti, K. et al. (2021) The distribution of glacial meltwater routes and associated murtoo fields in Finland. *Geomorphology*, 389, 107854. Available from: https://doi.org/10.1016/j.geomorph.2021.107854

Bartholomaus, T.C., Anderson, R.S. & Anderson, S.P. (2008) Response of glacier basal motion to transient water storage. *Nature Geoscience*, 1, 33–37. Available from: https://doi.org/10.1038/ngeo.2007.52

Bartholomew, I., Nienow, P., Mair, D., Hubbard, A., King, M.A. & Sole, A. (2010) Seasonal evolution of subglacial drainage and acceleration in a Greenland outlet glacier. *Nature Geoscience*, 3(6), 408–411. Available from: https://doi.org/10.1038/ngeo863

Batchelor, C.L., Margold, M., Krapp, M., Murton, D.K., Dalton, A.S., Gibbard, P.L. et al. (2019) The configuration of Northern Hemisphere ice sheets through the Quaternary. *Nature Communications*, 10, 3713. Available from: https://doi.org/10.1038/s41467-019-11601-2

Bennett, M. & Glasser, N. (2009) *Glacial Geology – Ice Sheet and Landforms*. Chichester: Wiley.

Bennett, M.R., Huddart, D. & Waller, R.I. (2006) Diamict fans in subglacial water-filled cavities—a new glacial environment. *Quaternary Science Reviews*, 25(21–22), 3050–3069. Available from: https://doi.org/10.1016/j.quascirev.2006.05.004

Björck, S. (1995) A review of the history of the Baltic Sea, 13.0–8.0 ka BP. *Quaternary International*, 27, 19–40. Available from: https://doi.org/10.1016/1040-6182(94)00057-C

Boulton, G. & Hindmarsh, R. (1987) Sediment deformation beneath glaciers: Rheology and geological consequences. *Journal of Geophysical Research*, 92(B9), 9059–9082. Available from: https://doi.org/10.1029/JB092iB09p09059

Boulton, G.S., Dongelmans, P., Punkari, M. & Broadgate, M. (2001) Palaeoglaciology of an ice sheet through a glacial cycle: The European ice sheet through the Weichselian. *Quaternary Science Reviews*, 20(4), 591–625. Available from: https://doi.org/10.1016/S0277-3791(00)00160-8

Bowling, J.S., Livingstone, S.J., Sole, A.J. & Chu, W. (2019) Distribution and dynamics of Greenland subglacial lakes. *Nature Communications*, 10, 2810. Available from: https://doi.org/10.1038/s41467-019-10821-w

Chandler, D.M., Wadham, J.L., Nienow, P.W., Doyle, S.H., Tedstone, A.J., Telling, J. et al. (2021) Rapid development and persistence of efficient subglacial drainage under 900 m-thick ice in Greenland. *Earth and Planetary Science Letters*, 566, 116982. Available from: https://doi.org/10.1016/j.epsl.2021.116982

Christoffersen, P., Tulaczyk, S., Wattrus, N.J., Peterson, J., Quintana-Krupinski, N., Clark, C.D. et al. (2008) Large subglacial lake beneath the Laurentide Ice Sheet inferred from sedimentary sequences. *Geology*, 36(7), 563–566. Available from: https://doi.org/10.1130/G24628A.1

Chu, W.T., Creyts, T. & Bell, R.E. (2016) Rerouting of subglacial water flow between neighboring glaciers in West Greenland. *Journal of Geophysical Research – Earth Surface*, 121(5), 925–938. Available from: https://doi.org/10.1002/2015JF003705

Clark, C.D., Hughes, A.L., Greenwood, S.L., Jordan, C. & Sejrup, H.P. (2012) Pattern and timing of retreat of the last British–Irish Ice Sheet. *Quaternary Science Reviews*, 44, 112–146. Available from: https://doi.org/10.1016/j.quascirev.2010.07.019

Clarke, G.K.C. (2005) Subglacial processes. *Review of Earth and Planetary Sciences*, 33(1), 247–276. Available from: https://doi.org/10.1146/annurev.earth.33.092203.122621

Clerc, S., Bouncristiani, J.-F., Guiraud, M., Desaubliaux, G. & Portier, E. (2012) Depositional model in subglacial cavities, Killiney Bay, Ireland: Interactions between sedimentation, deformation and glacial dynamics. *Quaternary Science Reviews*, 33, 142–164. Available from: https://doi.org/10.1016/j.quascirev.2011.12.004

Copland, L., Sharp, M.J. & Nienow, P. (2003) Links between short-term velocity variations and the subglacial hydrology of a predominantly cold polythermal glacier. *Journal of Glaciology*, 49(166), 337–348. Available from: https://doi.org/10.3189/172756503781830656

Cuffey, K.M. & Paterson, W.S.B. (2010) *The Physics of Glaciers*, 4th edition. Elsevier: Amsterdam.

Das, S.B., Joughin, I., Behn, M.D., Howat, I.M., King, M.A., Lizarralde, D. & Bhatia, M.P. (2008) Fracture propagation to the base of the Greenland Ice Sheet during supraglacial lake drainage. *Science*, 320(5877), 778–781. Available from: https://doi.org/10.1126/science.1153360

Davison, B.J., Sole, A.J., Livingstone, S.J., Cowton, T.R. & Nienow, P.W. (2019) The influence of hydrology on the dynamics of land-terminating sectors of the Greenland Ice Sheet. *Frontiers in Earth Sciences*, 7, 10. Available from: https://doi.org/10.3389/feart.2019.00010

De Geer, G. (1912) Geochronologie der letzten 12,000 Jahre. *Geologische Rundschau*, 3(7), 457–471. Available from: https://doi.org/10.1007/BF01802565

Doyle, S.H., Hubbard, B., Christoffersen, P., Law, R., Hewitt, D.R., Neufeld, J.A. et al. (2021) Water flow through sediments and at the ice–sediment interface beneath Sermeq Kujalleq (Store Glacier), Greenland. *Journal of Glaciology*, 1–20. Available from: https://doi.org/10.1017/jog.2021.121

Evans, DJA & Benn, D.I. (Eds). (2004) *A Practical Guide to the Study of Glacial Sediments*. New York: Oxford University Press.

Evans, D.J.A., Phillips, E.R., Hiemstra, J.F. & Auton, C.A. (2006) Subglacial till: Formation, sedimentary characteristics and classification. *Earth-Science Reviews*, 78(1–2), 115–176. Available from: https://doi.org/10.1016/j.earscirev.2006.04.001

Fenn, C.R., Gurnell, A.M. & Beecroft, I.R. (1985) An evaluation of the use of suspended sediment rating curves for the prediction of suspended sediment concentration in a proglacial stream. *Geografiska Annaler:*

Series A, Physical Geography, 67(1–2), 71–82. Available from: https://doi.org/10.1080/04353676.1985.11880131

Fricker, H.A., Scambos, T., Bindschadler, R. & Padman, L. (2007) An active subglacial water system in West Antarctica mapped from space. *Science*, 315(5818), 1544–1548. Available from: https://doi.org/10.1126/science.1136897

Garzanti, E., Andò, S. & Vezzoli, G. (2008) Settling equivalence of detrital minerals and grain-size dependence of sediment composition. *Earth and Planetary Science Letters*, 273(1–2), 138–155. Available from: https://doi.org/10.1016/j.epsl.2008.06.020

Gordon, S., Sharp, M., Hubbard, B., Smart, C., Ketterling, B. & Willis, I. (1998) Seasonal reorganisation of subglacial drainage inferred from measurements in boreholes. *Hydrological Processes*, 12(1), 105–133. Available from: https://doi.org/10.1002/(SICI)1099-1085(199801)12:1<105::AID-HYP566>3.0.CO;2-#

Håkanson, L. & Jansson, M. (1983) *Principles of Lake Sedimentology*. Berlin: Springer-Verlag.

Hall, A.M., Krabbendam, M., van Boeckel, M., Goodfellow, B.W., Hättestrand, C., Heyman, J. et al. (2020) Glacial ripping: Geomorphological evidence from Sweden for a new process of glacial erosion. *Geografiska Annaler: Series A, Physical Geography*, 102(4), 333–353. Available from: https://doi.org/10.1080/04353676.2020.1774244

Hart, J.K. (1995) Subglacial erosion, deposition and deformation associated with deformable beds. *Progress in Physical Geography*, 19(2), 173–191. Available from: https://doi.org/10.1177/030913339501900202

Hodder, K.R. & Gilbert, R. (2007) Evidence for flocculation in glacier-fed Lillooet Lake, British Columbia. *Water Research*, 41(12), 2748–2762. Available from: https://doi.org/10.1016/j.watres.2007.02.058

Hughes, A.L.C., Gyllencreutz, R., Lohne, Ø.S., Mangerud, J. & Svendsen, J.I. (2016) The last Eurasian ice sheets – a chronological database and time-slice reconstruction, DATED-1. *Boreas*, 45(1), 1–45. Available from: https://doi.org/10.1111/bor.12142

Iken A. & Bindschadler, R. (1986) Combined measurements of subglacial water pressure and surface velocity of Findelengletscher, Switzerland: conclusions about drainage system and sliding mechanism. *Journal of Glaciology*, 32, 101–119.

Kamb, B. (1987) Glacier surge mechanism based on linked cavity configuration of the basal water conduit system. *Journal of Geophysical Research*, B92, 9083–9100.

Kleman, J., Hättestrand, C., Borgström, I. & Stroeven, A. (1997) Fennoscandian palaeoglaciology reconstructed using a glacial geological inversion model. *Journal of Glaciology*, 43, 283–299.

Kuhn, G., Hillenbrand, C.-D., Kasten, S., Smith, J.A., Nitsche, F.O., Frederichs, T. et al. (2017) Evidence for a palaeo-subglacial lake on the Antarctic continental shelf. *Nature Communications*, 8(1), 15591. Available from: https://doi.org/10.1038/ncomms15591

Lahtinen, R. (1996) Geochemistry of Palaeoproterozoic supracrustal and plutonic rocks in the Tampere–Hämeenlinna area, southern Finland. *Geological Survey of Finland, Bulletin*, 389, 1–113.

Lesemann, J.-E., Alsop, G.I. & Piotrowski, J.A. (2010) Incremental subglacial meltwater sediment deposition and deformation associated with repeated ice-bed decoupling: A case study from the Island of Funen, Denmark. *Quaternary Science Reviews*, 29, 3212–3229.

Lesemann, J.-E., Alsop, G.I., & Piotrowski, J.A. (2011). Subglacial deposition and deformation of glaciofluvial sediments during episodic glacier-bed decoupling events. GeoHydro2011; GeoHydro Proceeding Papers, 1–7.

Lewington, E.L., Livingstone, S.J., Clark, C.D., Sole, A.J. & Storrar, R.D. (2020) A model for interaction between conduits and surrounding hydraulically connected distributed drainage based on geomorphological evidence from Keewatin, Canada. *The Cryosphere*, 14(9), 2949–2976. Available from: https://doi.org/10.5194/tc-14-2949-2020

Livingstone, S.J., Piotrowski, J.A., Bateman, M.D., Ely, J. & Clark, C. (2015) Discriminating between subglacial and proglacial lake sediments: An example from the Dänischer Wohld Peninsula, northern Germany. *Quaternary Science Reviews*, 112, 86–108.

Lunkka, J.P., Palmu, J.-P. & Seppänen, A. (2021) Deglaciation dynamics of the Scandinavian Ice Sheet in the Salpausselkä zone, southern Finland. *Boreas*, 50, 404–418. Available from: https://doi.org/10.1111/bor.12502

Mäkinen, J. (2003) Development of depositional environments within the interlobate Säkylänharju–Virttaankangas glaciofluvial complex in SW Finland. *Annales Academiae Scientiarum Fennicae, Series A3: Geologica Geographica*, 165, 1–65.

Mäkinen, J., Kajuutti, K., Ojala, A., Ahokangas, E., Palmu, J.-P. (2019). Sedimentary characteristics of Finnish MURTOOs – triangular-shaped subglacial landforms produced during rapid retreat of continental ice sheets. Advances in Glacier Hydrology III Posters, C13C-1309. AGU Fall Meeting San Francisco CA, 9–13 December 2019.

Mäkinen, J., Kajuutti, K., Palmu, J.-P., Ojala, A. & Ahokangas, E. (2017) Triangular-shaped landforms reveal subglacial drainage routes in SW Finland. *Quaternary Science Reviews*, 164, 37–53.

Malczyk, G., Gourmelen, N., Goldberg, D., Wuite, J. & Nagler, T. (2020) Repeat subglacial lake drainage and filling beneath Thwaites Glacier. *Geophysical Research Letters*, 47, e2020GL089658.

Mejia, J.Z., Gulley, J.D., Trunz, C., Covington, M.D., Bartholomaus, T.C., Xie, S. et al. (2021) Isolated cavities dominate Greenland Ice Sheet dynamic response to lake drainage. *Geophysical Research Letters*, 48(19), e2021GL094762. Available from: https://doi.org/10.1029/2021GL094762

Menzies, J., van der Meer, J.J.M. & Shilts, W.W. (2018) Subglacial processes and sediments. In: Menzies, J. & van der Meer, J.J.M. (Eds.) *Past Glacial Environments* (2nd edition, pp. 105–158). Elsevier: Amsterdam.

Möller, P. & Dowling, T.P.F. (2018) Equifinality in glacial geomorphology: Instability theory examined via ribbed moraine and drumlins in Sweden. *GFF*, 140, 106–135.

Munro-Stasiuk, M.J. (2003) Subglacial Lake McGregor, south-central Alberta, Canada. *Sedimentary Geology*, 160, 325–350.

Nienow, P.W., Sole, A.J., Slater, D.A. & Cowton, T.R. (2017) Recent advances in our understanding of the role of meltwater in the Greenland Ice Sheet system. *Current Climate Change Reports*, 3, 330–344.

Ojala, A.E.K., Heinsalu, A., Saarnisto, M. & Tiljander, M. (2005) Annually laminated sediments date the drainage of the Ancylus Lake and early Holocene shoreline displacement in central Finland. *Quaternary International*, 130, 63–73. Available from: https://doi.org/10.1016/j.quaint.2004.04.032

Ojala, A.E.K., Mäkinen, J., Ahokangas, E., Kajuutti, K., Valkama, M., Tuunainen, A. et al. (2021) Diversity of murtoos and murtoo-related subglacial landforms in the Finnish area of the Scandinavian Ice Sheet. *Boreas*, 50(4), 1095–1115. Available from: https://doi.org/10.1111/bor.12526

Ojala, A.E.K., Palmu, J.-P., Åberg, A., Åberg, S. & Virkki, H. (2013) Development of an ancient shoreline database to reconstruct the Litorina sea maximum extension and the highest shoreline of the Baltic sea basin in Finland. *Bulletin of the Geological Society of Finland*, 85, 127–144. Available from: https://doi.org/10.17741/bgsf/85.2.002

Ojala, A.E.K., Peterson, G., Mäkinen, J., Johnson, M., Kajuutti, K., Ahokangas, E. et al. (2019) Ice sheet scale distribution of unique triangular-shaped hummocks (murtoos) – a subglacial landform produced during rapid retreat of the Scandinavian Ice Sheet. *Annals of Glaciology*, 60(80), 115–126. Available from: https://doi.org/10.1017/aog.2019.34

Pajunen, H. (2004) Lake sediments as a store of dry matter and carbon. *Geological Survey of Finland, Report of Investigation*, 160, 1–308.

Palmu, J.-P., Ojala, A.E.K., Virtasalo, J., Putkinen, N. & Kohonen, J. (2021) Classification system of superficial (Quaternary) geologic units in Finland. *Geological Survey of Finland, Bulletin*, 412, 115–144.

Peterson Becher, G. & Johnson, M.J. (2021) Sedimentology and internal structure of murtoos – V-shaped landforms indicative of a dynamic subglacial hydrological system. *Geomorphology*, 380, 107644.

Powers, M.C. (1953) A new roundness scale for sedimentary particles. *Journal of Sedimentary Petrology*, 23, 117–119. Available from: https://doi.org/10.1306/D4269567-2B26-11D7-8648000102C1865D

Punkari, M. (1980) The ice lobes of the Scandinavian ice sheet during the deglaciation in Finland. *Boreas*, 9(4), 307–310. Available from: https://doi.org/10.1111/j.1502-3885.1980.tb00710.x

Rada, C. & Schoof, C. (2018) Channelized, distributed, and disconnected: Subglacial drainage under a valley glacier in the Yukon. *The*

Cryosphere, 12(8), 2609–2636. Available from: https://doi.org/10.5194/tc-12-2609-2018

Rainio, H., Saarnisto, M. & Ekman, I. (1995) Younger Dryas end moraines in Finland and NW Russia. *Quaternary International*, 28, 179–192.

Ravier, E., Buoncristiani, J.-F., Clerc, S., Guiraud, M., Menzies, J. & Portier, E. (2014) Sedimentological and deformational criteria for discriminating subglaciofluvial deposits from subaqueous ice-contact fan deposits: A Pleistocene example (Ireland). *Sedimentology*, 61(5), 1382–1410. Available from: https://doi.org/10.1111/sed.12111

Rinterknecht, V., Hang, T., Gorlach, A., Kohv, M., Kalla, K., Kalm, V. et al. Guillou, V. (2018) The Last Glacial Maximum extent of the Scandinavian Ice Sheet in the Valday Heights, western Russia: Evidence from cosmogenic surface exposure dating using ^{10}Be. *Quaternary Science Reviews*, 200, 106–113. Available from: https://doi.org/10.1016/j.quascirev.2018.09.032

Röthlisberger, H. (1972) Water pressure in intra- and subglacial channels. *Journal of Glaciology*, 11(62), 177–203. Available from: https://doi.org/10.3189/S0022143000022188

Sauramo, M. (1923) Studies on the Quaternary varve sediments in southern Finland. *Bulletin de la Commission Géologique de Finlande*, 60, 1–164.

Shaw, J. (1982) Melt out till in the Edmonton area, Alberta, Canada. *Canadian Journal of Earth Sciences*, 19(8), 1548–1569. Available from: https://doi.org/10.1139/e82-134

Skidmore, M.L. & Sharp, M.L. (1999) Drainage system behaviour of a high Arctic polythermal glacier. *Annals of Glaciology*, 28, 209–215. Available from: https://doi.org/10.3189/172756499781821922

Stroeven, A.P., Hättestrand, C., Kleman, J., Heyman, J., Fabel, D., Fredin, O. et al. (2016) Deglaciation of Fennoscandia. *Quaternary Science Reviews*, 147, 91–121.

Sundal, A.V., Shepherd, A., Nienow, P., Hanna, E., Palmer, S. & Huybrechts, P. (2011) Melt-induced speed-up of Greenland ice sheet offset by efficient subglacial drainage. *Nature*, 469(7331), 521–524. Available from: https://doi.org/10.1038/nature09740

Svendsen, J.I., Alexanderson, H., Astakhov, V.I., Demidov, I., Dowdeswell, J.A., Funder, S. et al. (2004) Late Quaternary ice sheet history of northern Eurasia. *Quaternary Science Reviews*, 23(11–13), 1229–1271. Available from: https://doi.org/10.1016/j.quascirev.2003.12.008

Troels-Smith, J. (1955) Characterisation of unconsolidated sediments. *Geological Survey of Denmark*, IV3(10), 1–73. Available from: https://doi.org/10.34194/raekke4.v3.6989

Virtasalo, J.J., Hämäläinen, J. & Kotilainen, A.T. (2014) Toward a standard stratigraphical classification practice for the Baltic Sea sediments: The CUAL approach. *Boreas*, 43, 924–938. Available from: https://doi.org/10.1111/bor.12076

Willis, I.C., Arnold, N.S. & Brock, B.W. (2003) Effect of snowpack removal on energy balance, melt and runoff in a small supraglacial catchment. *Hydrological Processes*, 16(14), 2721–2749. Available from: https://doi.org/10.1002/hyp.1067

Winterhalter, B. (1992) Late-Quaternary stratigraphy of Baltic Sea sediments – a review. *Bulletin of the Geological Society of Finland*, 64(2), 189–194. Available from: https://doi.org/10.17741/bgsf/64.2.007

Zolitschka, B., Francus, P., Ojala, A.E.K. & Schimmelmann, A. (2015) Varves in lake sediments – a review. *Quaternary Science Reviews*, 117, 1–41.

SUPPORTING INFORMATION

Additional supporting information can be found online in the Supporting Information section at the end of this article.

How to cite this article: Ojala, A.E.K., Mäkinen, J., Kajuutti, K., Ahokangas, E., Palmu, J.-P. (2022) Subglacial evolution from distributed to channelized drainage: Evidence from the Lake Murtoo area in SW Finland. *Earth Surface Processes and Landforms*, 1–20. Available from: https://doi.org/10.1002/esp.5430